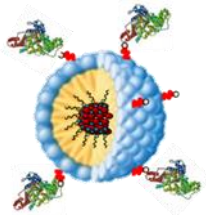

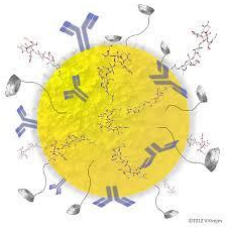

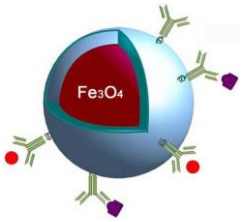

Current Drug Metabolism,
Volume 17 , Issue 8 , 2016

New Metal based nanoparticles coated with biomolecules for targeted therapy

Dr. Laura Zaccaro
Istituto di Biostrutture e Bioimmagini-CNR-Napoli
lzaccaro@unina.it

Scuola di Bioinorganica, CNR-Roma 13-15 febbraio 2019

Overview

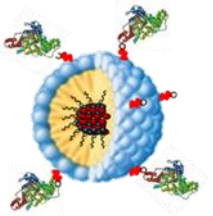

- Cancer and Targeted therapy
- Nanotechnology in Targeted Therapy
- Magnetic and Gold Nanoparticles
- New Metallic Nanopartcles as Theranostics

Cancer and Targeted Therapy

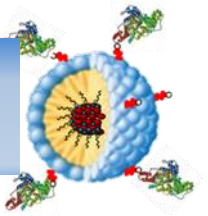

- Cancer is currently one of the most difficult global healthcare problem
- Standard treatments include chemotherapy, radiation, and surgery, but the effects of these procedures may damage not only the tumor tissue but also normal tissue.
- Cancer recurrence is believed to be one of the major reasons for the failure of cancer treatment strategies.
- Current problems in treating cancer include rapid drug clearance and biodegradation, and limited targeting.

The advent of nanomedicines have led significant advances in the field of targeted therapy

Advantages of therapeutic nanoparticles

- Revert unfavorable physicochemical properties of bioactive molecules to desirable biopharmacologic profiles;
- Improve delivery of therapeutics across biological barriers and compartments;
- Control release of bioactive agents;
- Enhance therapeutic efficacy by selective delivery of therapeutics to biological targets;
- Perform theranostic functions by combining multimodal imaging and simultaneous diagnosis and therapy into multifunctional nanoplatforms.

Nanomedicines in cancer treatament

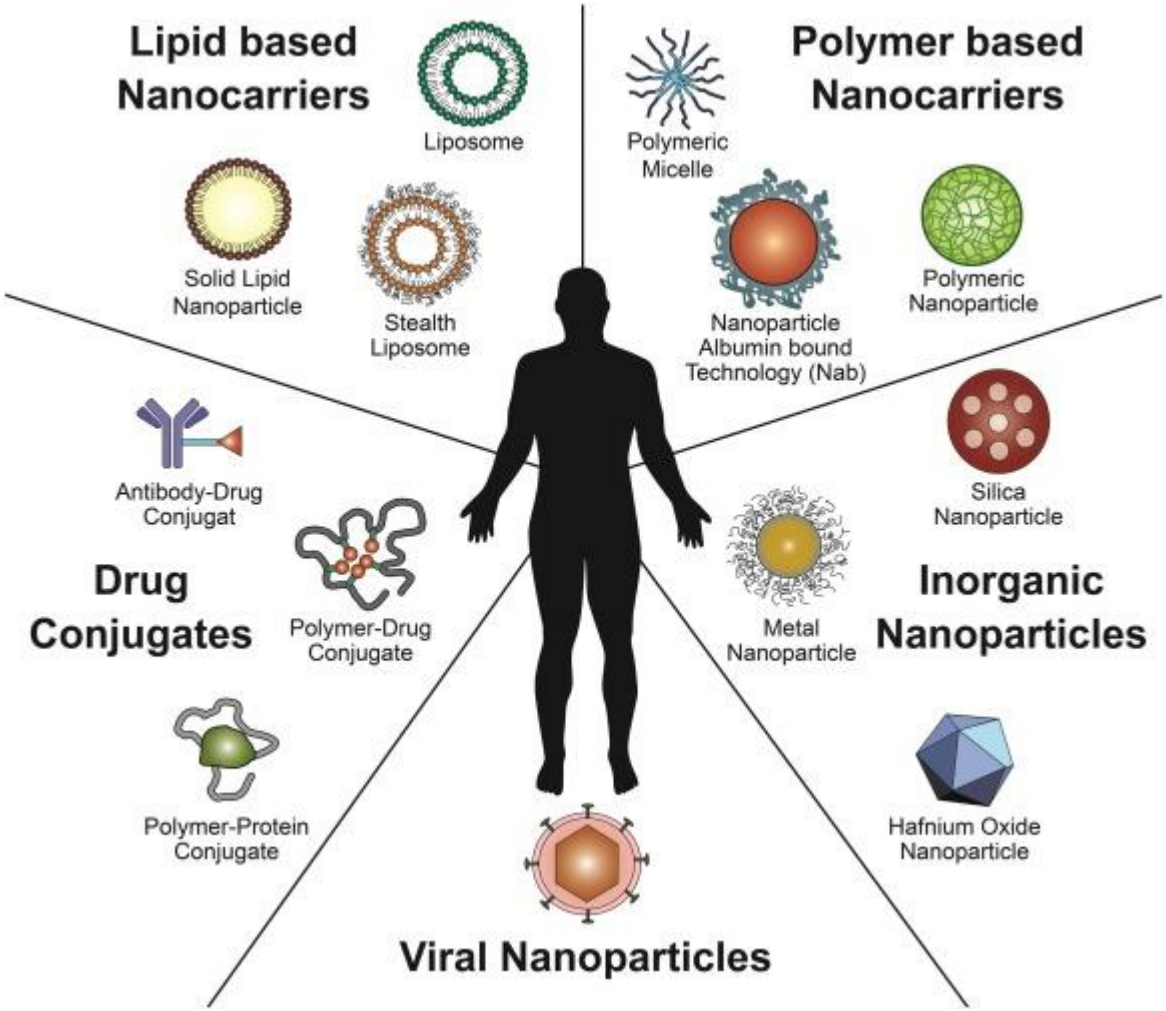

Tran et al. Clin Trans Med (2017) 6:44

Approved nanomedicines in the clinic

Year approved	Name	Type	Active drug	Diameter (references)	Type of cancer
Japan (1994)	Zinostatin stimalamer	Polymer protein conjugate	Styrene maleic anhydride neocarzinostatin (SMANCS)	*	Renal cancer
FDA (1995) EMA (1996)	Doxil/caelyx	Liposome (PEGylated)	Doxorubicin	80–90 nm [82]	HIV-associated Kaposi's sarcoma, ovarian cancer, metastatic breast cancer, multiple myeloma
FDA (1996)	DaunoXome	Liposome (non-PEGylated)	Daunorubicin	45 nm [83]	HIV-associated Kaposi's sarcoma
Taiwan (1998)	Lipo-Dox	Liposome	Doxorubicin	180 nm [84]	Kaposi's sarcoma, breast and ovarian cancer
FDA (1999)	DepoCyt	Liposome	Cytosine arabinoside (cytarabine)	10–20 μm [84]	Neoplastic meningitis
EMA (2000)	Myocet	Liposome	Doxorubicin	190 nm [84]	Breast cancer
FDA (2005) EMA (2008)	Abraxane	Nanoparticle albumin bound	Paclitaxel	130 nm [27]	Advanced non-small-cell lung cancer, metastatic pancreatic cancer, metastatic breast cancer
FDA (2006)	Oncaspar	PEG protein conjugate	L-Asparaginase	50–200 nm [84]	Leukemia
South Korea (2007)	Genexol-PM	PEG-PLA polymeric micelle	Paclitaxel	20–50 nm [85]	Breast cancer, Lung cancer, Ovarian cancer [126]
EMA (2009)	MEPACT	Liposome (non-PEGylated)	Mifamurtide	*	Osteosarcoma
EMA (2010)	NanoTherm	Iron oxide nanoparticle	–	20 nm [86]	Thermal ablation glioblastoma
FDA (2012)	Marqibo	Liposome (non-PEGylated)	Vincristine	100 nm [87]	Philadelphia chromosome negative acute lymphoblastic leukemia
FDA (2015)	MM-398 (Onivyde)	Liposome (PEGylated)	Irinotecan	80–140 nm [88]	Metastatic pancreatic cancer (2nd line)

* Data could not be found

Tran et al. Clin Trans Med (2017) 6:44

Nanoparticle Properties

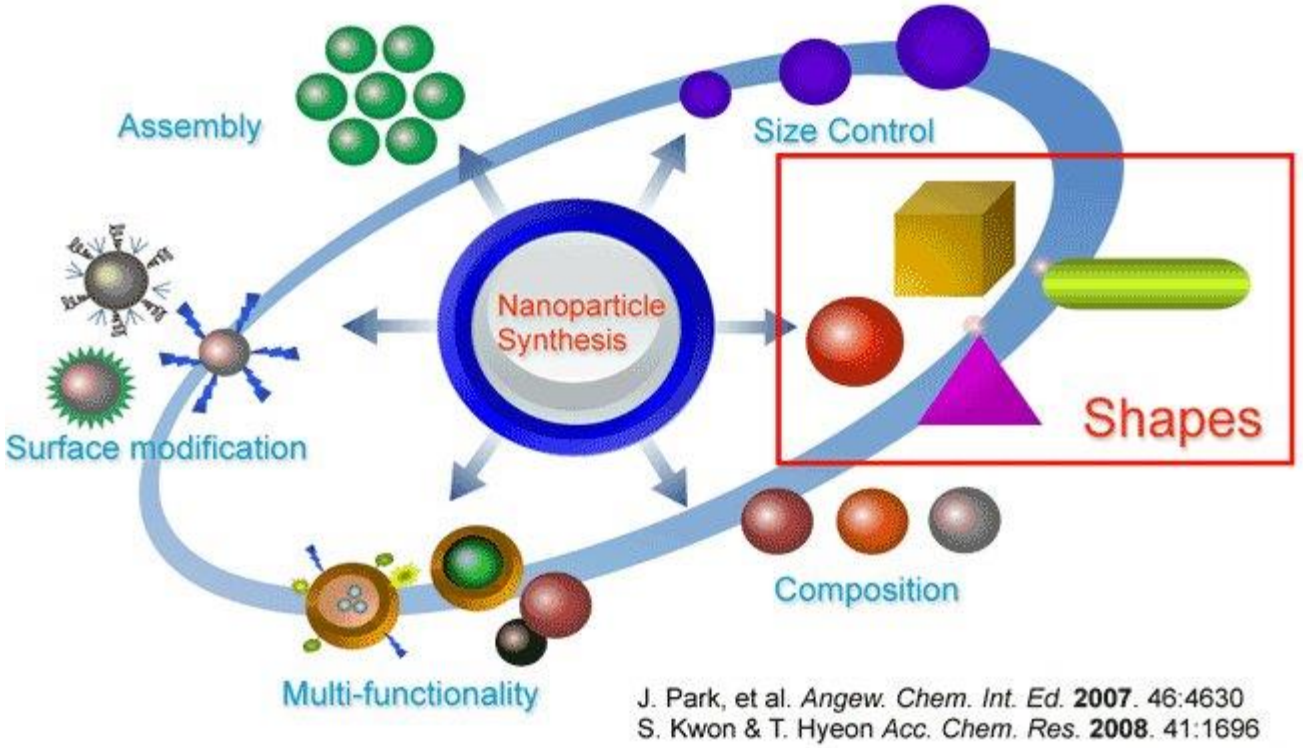

J. Park, et al. *Angew. Chem. Int. Ed.* **2007**. 46:4630
S. Kwon & T. Hyeon *Acc. Chem. Res.* **2008**. 41:1696

The properties of nanocarriers, including their nanoscale sizes, high surface-to-volume ratios, favorable drug release profiles, and targeting modifcations, can allow them to better reach target tumor tissue and release drugs in a stable, controlled manner

Surface features

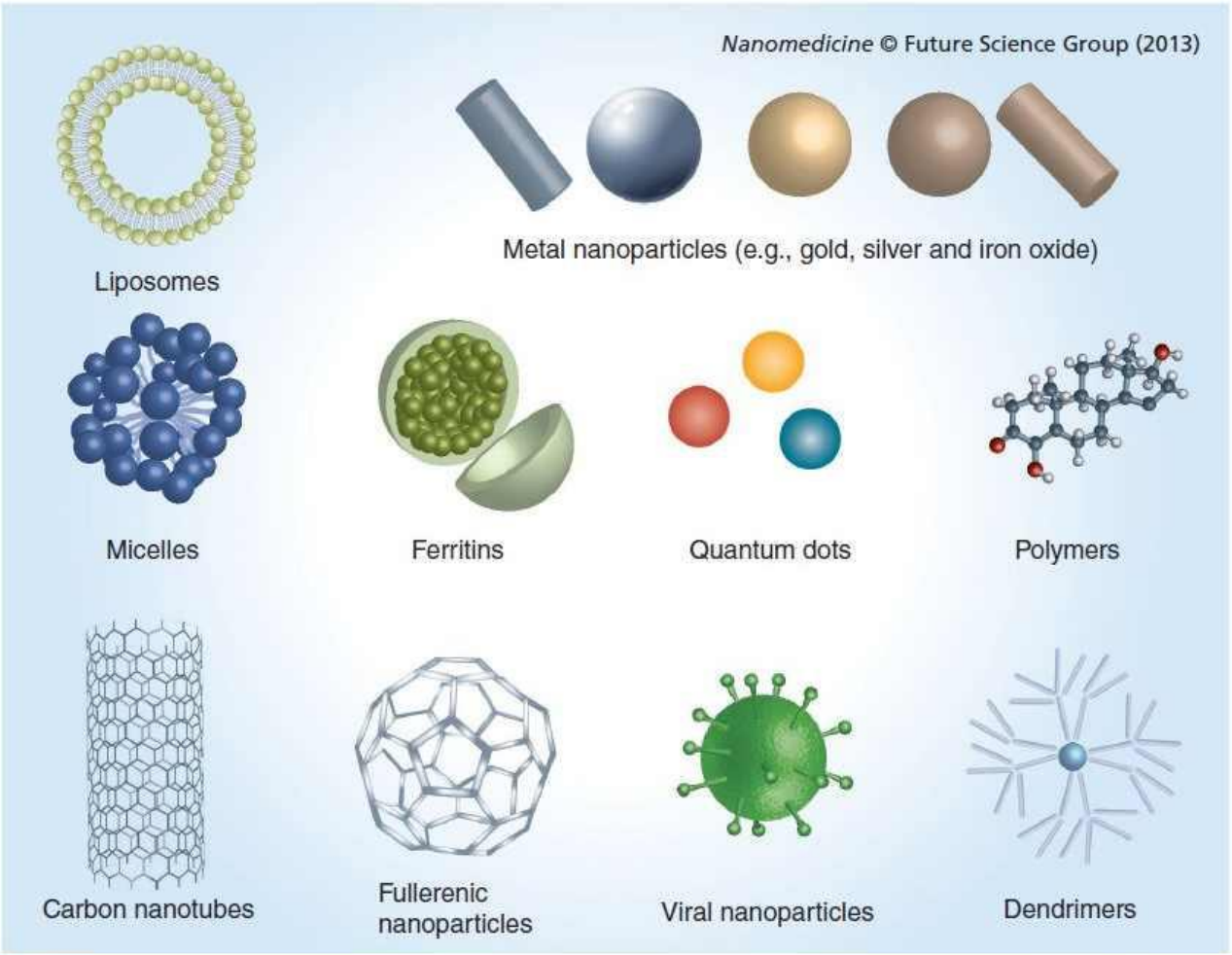

Nanoparticle size and shape

The shape and the size have high impact on:

- ❖ cell internalization mechanism
- ❖ high surface-to-volume ratios
- ❖ Optical and magnetic properties

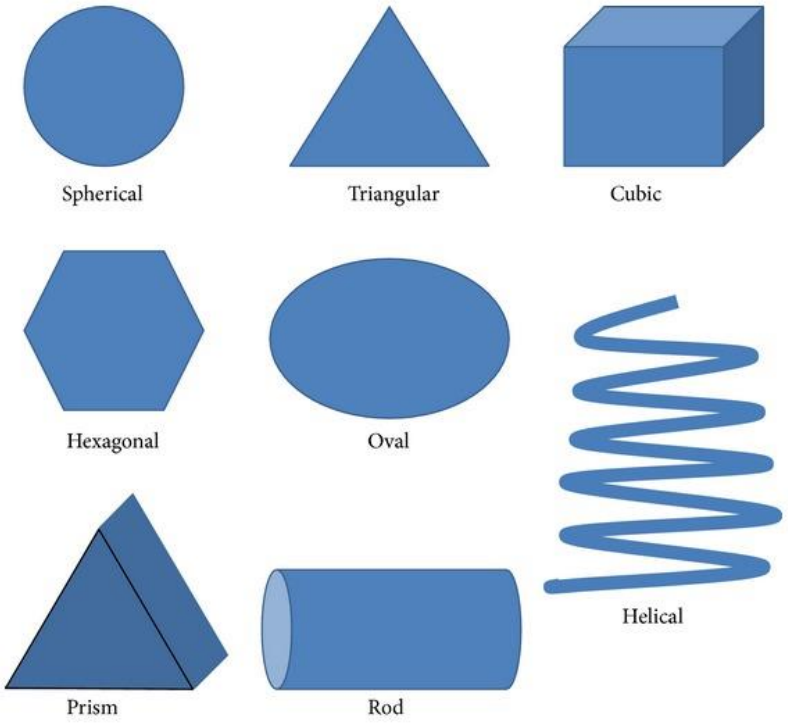

Surface features

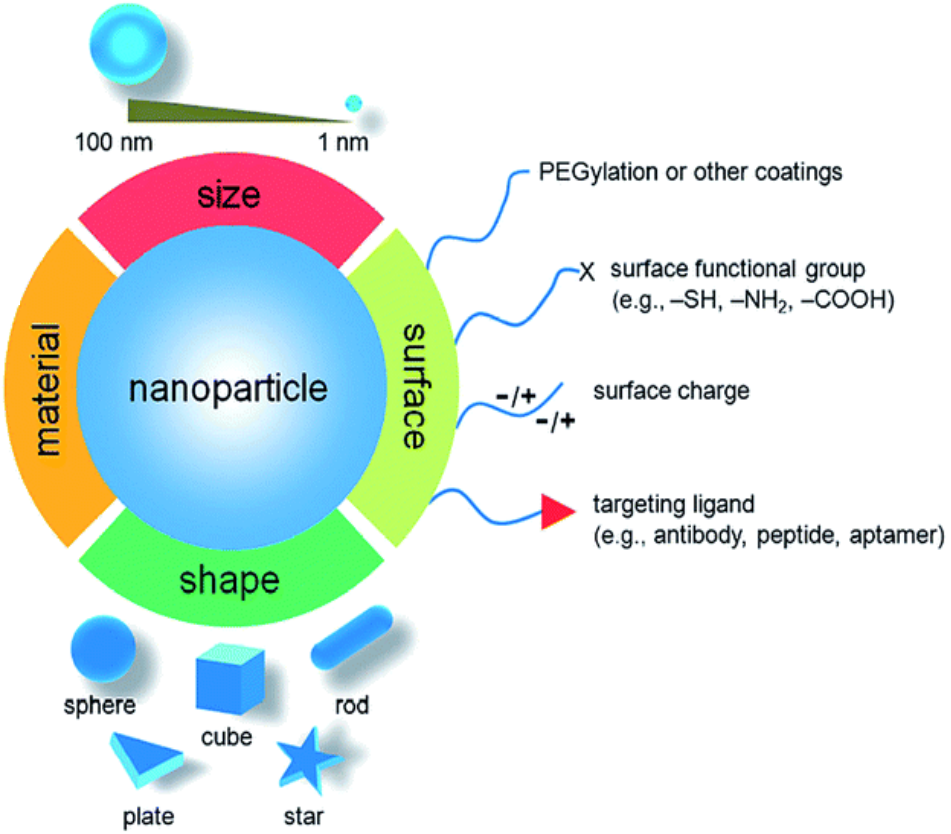

RSC Adv., 2016, 6, 82596–82615

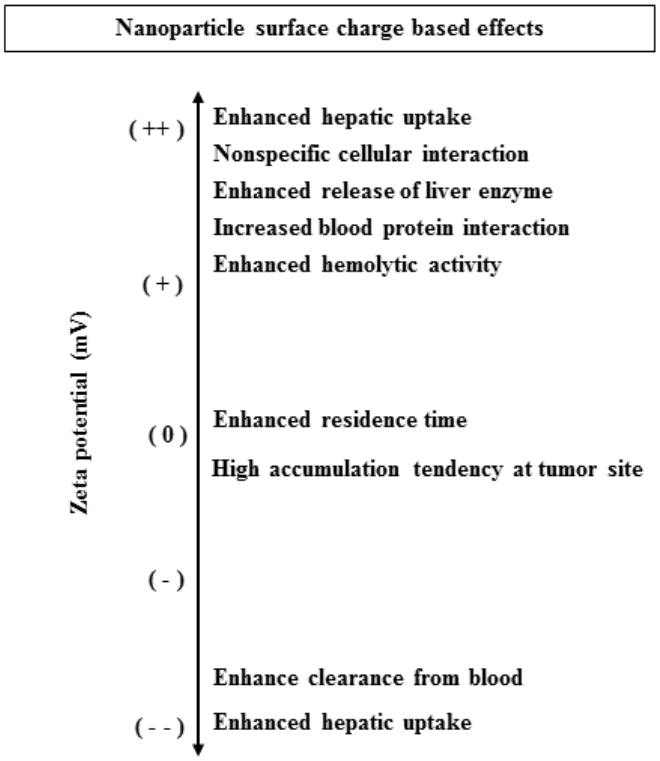

Synthetic methods

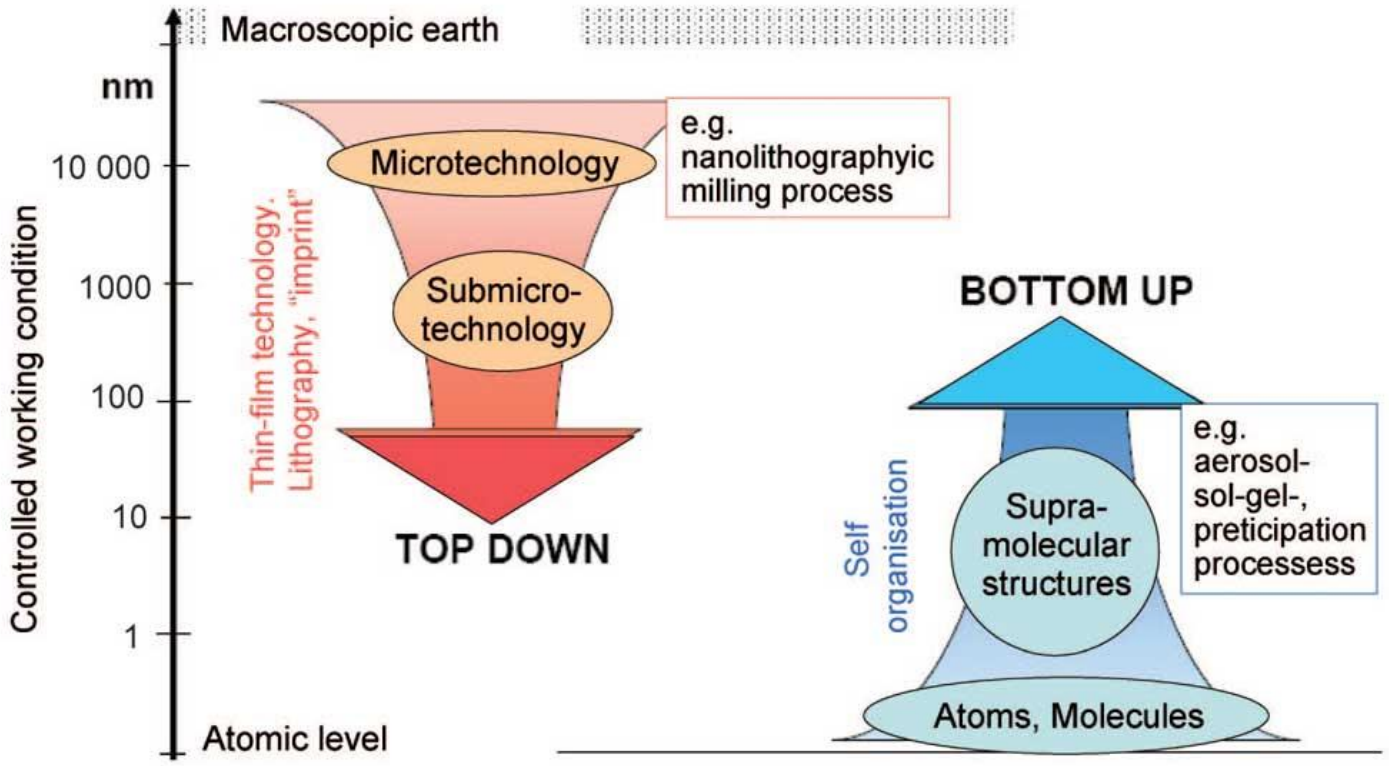

(Image: Laboratory for Micro and Nanotechnology, Paul Scherrer Institut)

Top-down or destructive method is the reduction of a bulk material to nanometric scale particles. Mechanical milling, nanolithography, laser ablation, sputtering and thermal decomposition are some of the most widely used nanoparticle synthesis methods

Bottom-up or constructive method is the build-up of material from atom to clusters to nanoparticles. Sol-gel, spinning, chemical vapour deposition (CVD), pyrolysis and biosynthesis are the most commonly used bottom-up methods for nanoparticle production.

Methods of Nanoparticle Synthesis

Physical Methods

High Energy Ball Milling
Metal NPs (Fe, Co), Inter-metallic NPs (FeCo, $CeCo_5$, $Nd_2Fe_{14}B$) , Single Crystal NPs (Sm_2Co_{17}) (Metal Oxides/Ferrites/ Carbonates NPs (ZnO, Fe_3O_4, $CoFe_2O_4$, $LiNbO_3$, $CaCO_3$), Carbon NPs (Graphite, Pure Carbon)

Inert Gas Condensation
Metal NPs (Cu, Ag, Au, Pt, Mn), Inter-metallic NPs (AuPd) , Core-Shell NPs (FeAg (core)-Si (shell))

Pulse Vapor Deposition
Sputtering
Metal NPs (Au, Ag, Co, Pt, Fe, Y), Metal Oxide (TiO_2, ZnO), Semiconducting (Ge), Magnetic (Fe-Pt), Hybrid (ZnS:Mn), Quantum Dots (Ge)

Electron Beam Evaporation
Metal NPs (Au, Ag, Pt), Inter-Metallic (Co-Pt), Composites (Pt-MWCNT, CoPt-Graphene)

Laser Ablation/Pulse Laser Deposition
Metal NPs (Ag, Fe, Ni, Se), Magnetic NPs (FeCo, FePt), Metal Sulphide (PbS), Metal Oxides(ZnO)

Vacuum Arc
Metal NPs (Ag, Fe, Au), Metallic Alloys (Mg-Al, Fe-Sn), Metal Sulphide (PbS), Metal Oxides(ZrO_2), Carbon NPs

Laser Pyrolysis
Metal Oxide NPs (TiO_2, SiO_2, Al_2O_3, Fe_2O_3), Non-Oxide NPs (Si, SiC, Si_3N_3, MoS_2) ,Ternary Composites NPs (Si/C/N, Si/Ti/C), Carbon based NPs (CN, C), Quantum Dots (Si)

Flash Spray Pyrolysis
Ceramic Oxide NPs (TiO_2, SiO_2, Al_2O_3, CeO2, MgO, CaO, WO_3/TiO_2), Ceramic Non-Oxide NPs ($BaCO_3$, $CaCO_3$, $CaSO_4$) , Metal Doped NPs (Fe Doped CeO_2, Pt Doped Zn_2TiO_4)

Electrospraying
Metal NPs (Au, Ag, Ti, Ni), Ceramic Oxide NPs (TiO_2, SiO_2, Al_2O_3, ZrO_2), Polymeric NPs (PLGA, PLA, Collagen, PMMA, PCL, Chitosan etc.)

Melt Mixing
Nanocomposite NPs (Polypyrrole-Polypropylene etc).

Biological Methods

Microorganisms Assisted Biogenesis
Metal NPs (Au, Ag, Hg, Cu, Pt, Pd), Metal oxide NPs (TiO_2, SiO_2, ZrO_2), Metal Sulphide NPs (CdS, PbS), Magnetite NPs, Quantum Dots (CdS, CdTe).

Bio-Templates Assisted Biogenesis
Metal NPs (Au, Ag, Pt)

Plant Extracts Assisted Biogenesis
Metal NPs (Au, Ag, Pt, Pd)

Chemical Methods

Sol-Gel Synthesis
Metal oxide NPs (ZnO, SnO_2, Fe_2O_3, Ta_2O_5), Ceramic NPs (TiO_2, SiO_2), NPs of CdSe, ZnB_2, $GdVO_4$ and Metal Aluminates, Magnetic NPs (Fe-Co)

Microemulsion Technique
Inorganic NPs:- Metal NPs (Au, Ag, Cu, Ni, Pt, Pd, Rh, Ir), semiconducting metal sulphite NPs (CdS, PbS, CuS, Cu_2S and CdSe), metal salt NPs ($BaCO_3$, $CaCO_3$ and $SrCO_3$), metal oxide NPs (ZrO_2, TiO_2, SiO_2, GeO_2 and Fe_2O_3), magnetic NPs ($(Mn,Zn)Fe_2O_4$, $(Ni,Zn)Fe_2O_4$, $ZnFe_2O_4$ and $BaFe_{12}O_{19}$) and composite nanoparticles (CdS-TiO_2, CdS-ZnS, CdS-SnO_2, CdS-SiO_2).
Organic NPs:- Polymers (Latex, Polystyrene, PMMA), Conducting Polymers (Polyaniline, Polypyrrole, Polythiophene), Organic molecules (Cholesterol, Retinol, Rhodiarome, Rhovanil)

Hydrothermal Synthesis
Metal NPs (Pt, Ag, Zr), Metal oxide NPs (ZnO, NiO, Fe_3O_4, CuO, α-Fe_2O_3), Metal Sulphide NPs (CdS), NPs of $CoFe_2O_4$, $FeWO_4$, $La_{1-x}Sr_xCrO_3$

Polyol Synthesis
Metal NPs (Ag, Pt, Cu, Pd, Pr), metal oxide NPs (ZnO, Indium-tin-oxide, Gd_2O_3, Cu_2O, Pr_6O_{11}), magnetic NPs (Fe_3O_4) and metal hybrid NPs ($CoSb_3$, FeCo).

Chemical Vapor Synthesis
Metal Oxide NPs (CoO, SiO_2, ZnO, Fe_2O_3), WS_2 NPs, Cu-Si/SiO_2 NPs, NPs of Al doped ZnO, fluorine doped tin oxide and Cr doped ZnO.

Plasma Enhanced Chemical Vapor Deposition
Carbon and Silicon NPs, Silica NPs, GaN NPs

RSC Adv., 2015, **5**, 105003-105037

Clinically relevant nanoparticle types

(Black: Approved Application, Red: Application in a Current Clinical Trial)

Organic

(a)

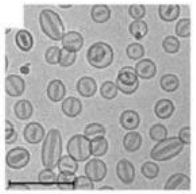

Liposomes:
Small-molecule Cancer Drugs
Ultrasound Contrast Agents
Vaccines
Anesthetics
Fungal Treatments
Macular Degeneration
Gene Therapies
Bacterial Infections
Inflammation (Arthritis)
Graft versus Host Disease

(b)

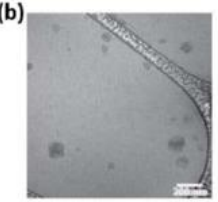

Protein-Based:
Small-molecule Cancer Drugs
Ultrasound Contrast Agents

(c)

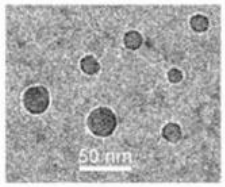

Polymeric/Micelle:
Small-molecule Cancer Drugs
Acute Radiation Syndrome

Inorganic

(d)

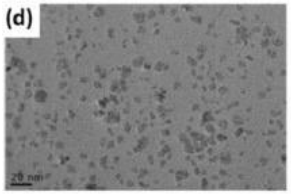

Iron-Oxide:
Anemia Therapies
Imaging Applications
Thermal Ablation of Tumors

(e)

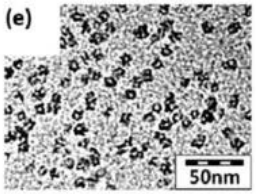

Silica:
Cancer Imaging

(f)

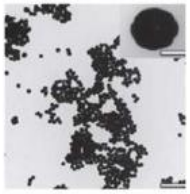

Gold:
Thermal Ablation of Tumors

Bioengineering & Translational Medicine 2016; 1: 10-29

Advantages versus disadvantages

Types of carriers	Advantages	Disadvantages
Liposomes	Biocompatible Longer duration of circulation Amphiphilic	May trigger immune response
Carbon nanoparticles	Multiple functions Chemical modification Water soluble and biocompatible Efficient loading	Toxicity
Polymeric micelles	Efficient carrier system for hydrophilic drug Biodegradable, self-assembling and biocompatible Potential targeting Functional modification	Occasional cytotoxicity Need of surface modifications
Dendrimers	Uniformity in size, shape and branch length Tuned pharmacokinetics and biodistribution Increased surface area, increased loading Targeting is achieved	Complex synthetic route
Metallic nanoparticles Gold nanoshells	Uniformity in size, shape and branch length Tuned pharmacokinetics and biodistribution Increased surface area, increased loading Targeting is achieved	Toxicity

Lambert M. et al , 2014, Expert.Opin.Drig Deliv, 11, 1087

Targeting for nanoparticle delivery

a Passive Targeting

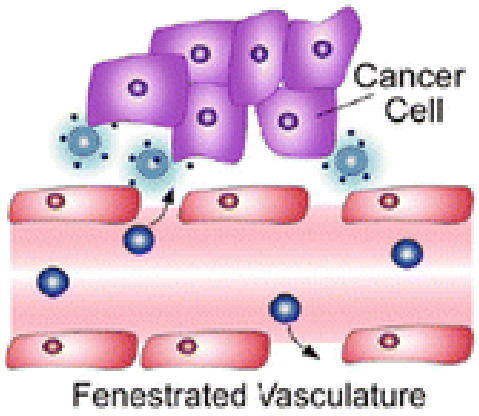

Passive targeting relies on the leaky vasculature that is exhibited by tumors, allowing nanoparticles to travel through the fenestrations and reach tumors.

b Active Targeting

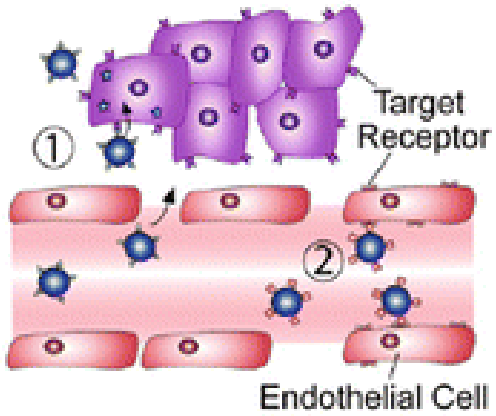

Active targeting can be used when nanoparticles have ligands on their surface that can recognize and bind receptors that are overexpressed on tumor cells.

c Triggered Release

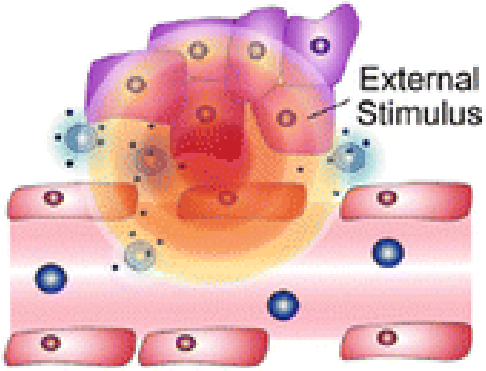

Tran et al. Clin Trans Med (2017) 6:44

Triggered release allows nanoparticles to congregate if exposed to an external stimulus such as a magnetic field or light

Active Targeting

Targeting nanoparticles to receptors or other surface membrane proteins overexpressed on target cells.

EGFR (epidermal growth factor) receptor overexpressed in malignant epithelial tumors as pancreatic and colerectal carcinoma

HER2 (human epidermal growth factor 2) receptor overexpressed in 25% of invasive cancer

PSMA (Prostate-specific membrane antigen) expressed on prostate cancer cells and on neovasculature of non prostate solid tumor

Transferrin receptor overexpressed on metastatic and drug resistant malignant cells

Integrin receptors overexpressed in activated neovessel and on cancer cell of solid tumors

Targeting ligands for active targeting

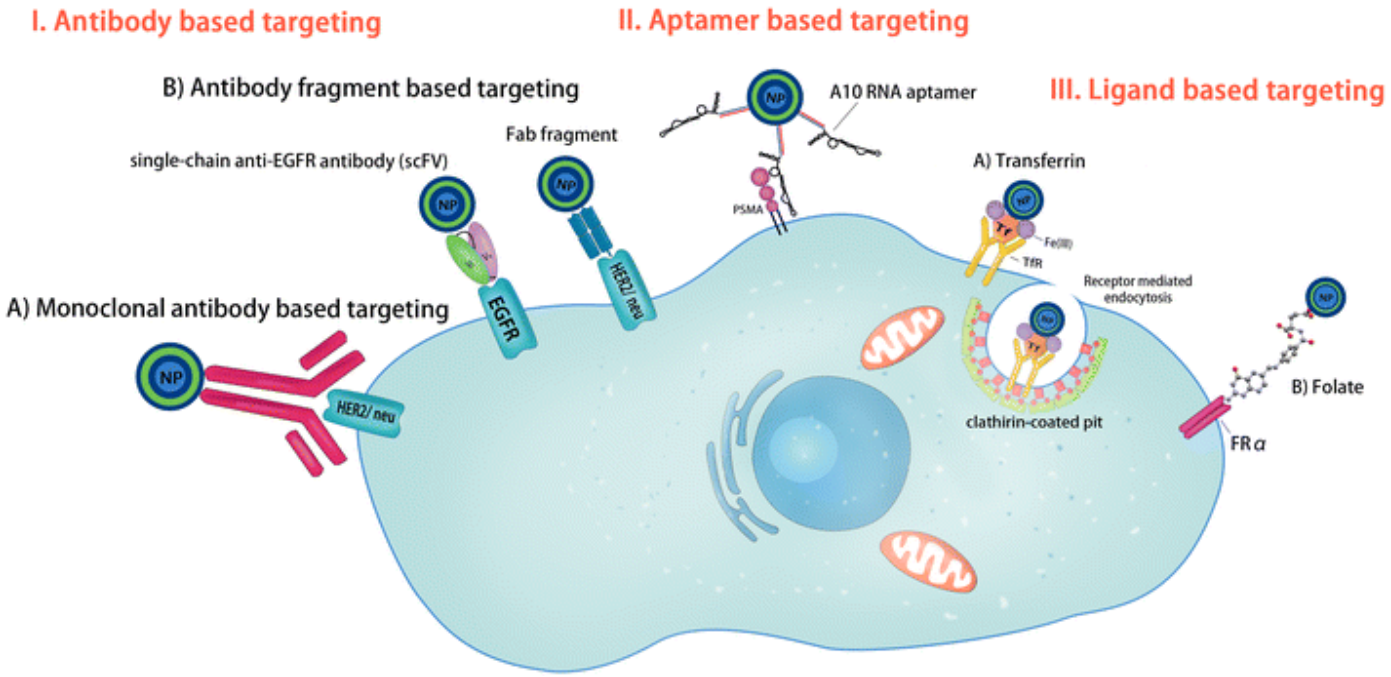

Bazak R et a. 2015, J cancer Res Clin Oncol, 141,769

Numerous targeting ligands have been employed to actively target nanoparticles including antibodies, antibody fragments, aptamers, peptides and whole proteins

Targeted Nps for cancer therapy

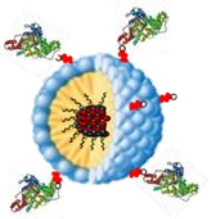

BIND-014:nanoparticles loaded with docetaxel and decorated with urea-based Inhibitor to bind PSMA (Phase II clinical trials)

Nanoparticles (PLA/PEG) loaded with docetaxel and decorated with RNA A10-aptamer to bind PSMA

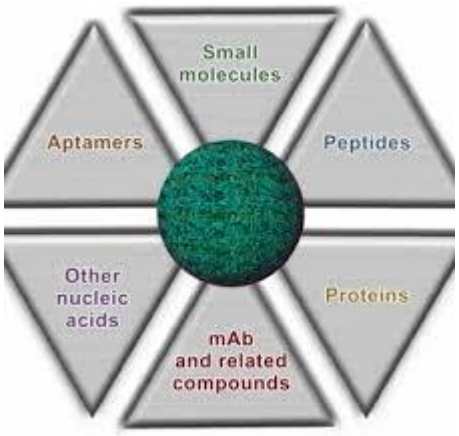

C-Dot: PEG- silica nanoparticles docorated with *i*RGD peptide

MBP-426, a scFv-transferrin-targeted liposome encapsulating oxaliplatin, that has been used clinically for the treatment of a variety of solid tumors.

Metallic Nanoparticles

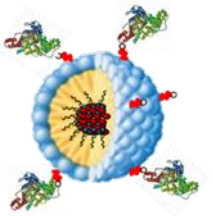

Metallic nanoparticles have unique characteristics such as magnetic and optical properties

targeted drug delivery

diagnostic imaging

THERANOSTIC AGENT

magnetic (Fe_3O_4) and gold nanoparticle

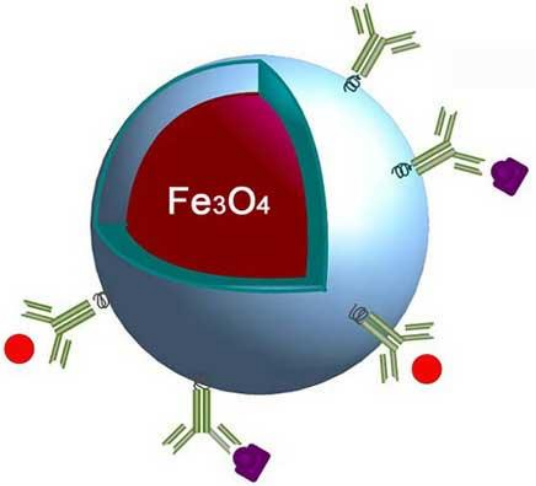

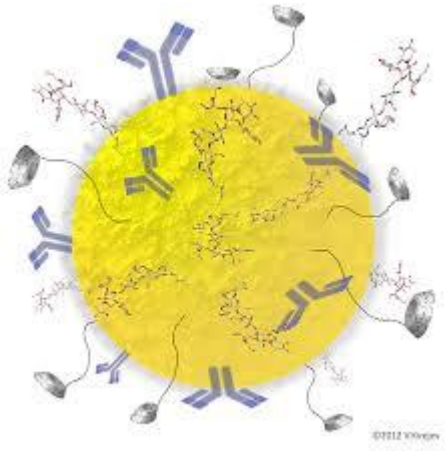

Current Drug Metabolism,
Volume 17 , Issue 8 , 2016

Magnetic nanoparticles (MNP)

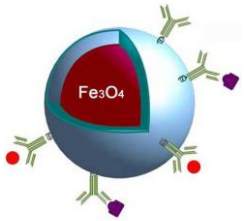

Current Drug Metabolism,
Volume 17 , Issue 8 , 2016

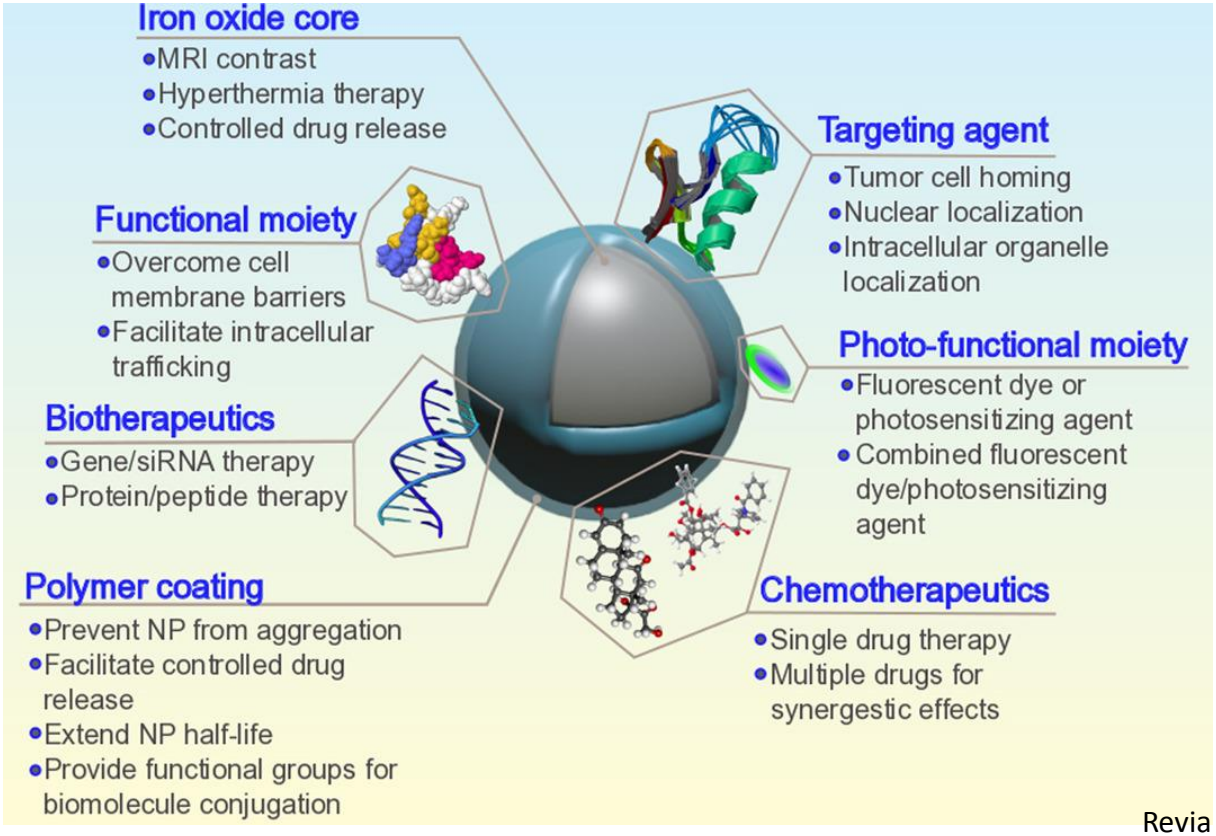

Revia RA et al. Materials Today
Volume 19,Number 3 April 2016

The most frequently used nanomaterial is the iron oxide nanoparticle, including magnetite (Fe_3O_4) and maghemite (γ-Fe_2O_3).

MNPs are generally in the superparamagnetic state (< 20 nm) (SPION)

MNP: synthesis methods

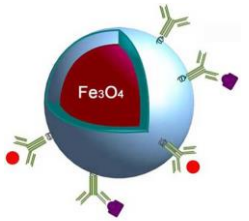

Current Drug Metabolism,
Volume 17 , Issue 8 , 2016

SPION are synthesized using a wide range of methods

Coprecipitation does not allow for good control of particle geometry and size distribution.

thermal decomposition in the oil phase can produce high-quality hydrophobic iron oxide NPs with perfect monodispersity and high crystallinity

microemulsion technique has the advantage of controlling the size of NPs by acting as a nanoreactor.

hydrolysis method and microwave-assisted synthesis produce NPs showing good water dispersibility and low cytotoxicity in the way of hydrolysis

Two main surface-modification strategies are able to improve the water dispersibility of SPION: (i) a ligand exchange process in order to replace original hydrophobic ligands and (ii) surface encapsulation with amphiphilic polymers

MNP: applications

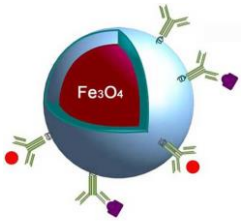

Current Drug Metabolism, Volume 17 , Issue 8 , 2016

Formulations of SPIONS already gained approval by the Food and Drug administration (FDA) in clinic as:

- ✓ **iron deficiency therapeutics (Feraheme)**
- ✓ **as MRI contrast agents(Gastromark)**

Development of the MNP also for:

- ✓ **Targeted MRI contrast agents**
- ✓ **Multimodal imaging**
- ✓ **Therapeutic treatment**
- ✓ **Monitoring cancer treatment in an efficient and effective manner**
- ✓ **Theranostic platforms**

SPIONs for targeted MRI imaging

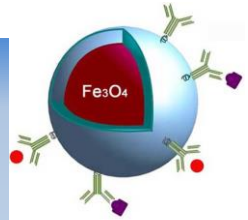

Current Drug Metabolism, Volume 17 , Issue 8 , 2016

Transferrin-conjugated superparamagnetic iron oxide nanoparticles (Tf-SPIONs), in rat brain glioma models.

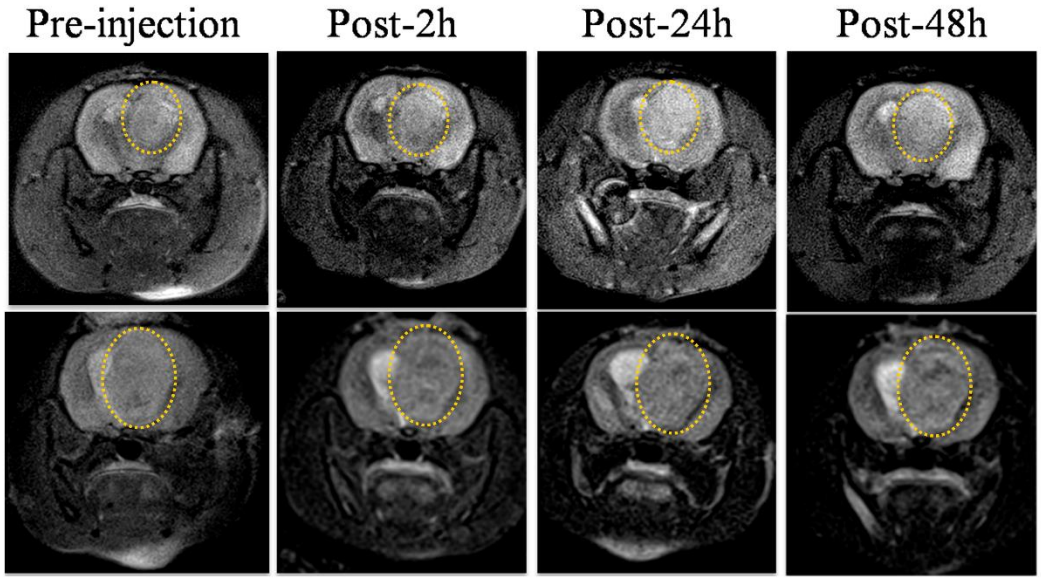

SPIONs (12 mg/kg);

Tf-SPIONs (12 mg/kg);

Jiang W et al., PlosOne 2012, 5 , e37376

The changing area of decreased MR signal intensity increased gradually with timing up to 48 h in comparison to the preinjection image of tumor.

MNP: Multimodal imaging

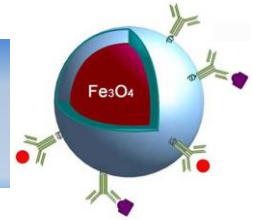

Current Drug Metabolism,
Volume 17 , Issue 8 , 2016

Multifunctional probe for targeting avb3 integrin and multimodal imaging of cancer cells simultaneously.

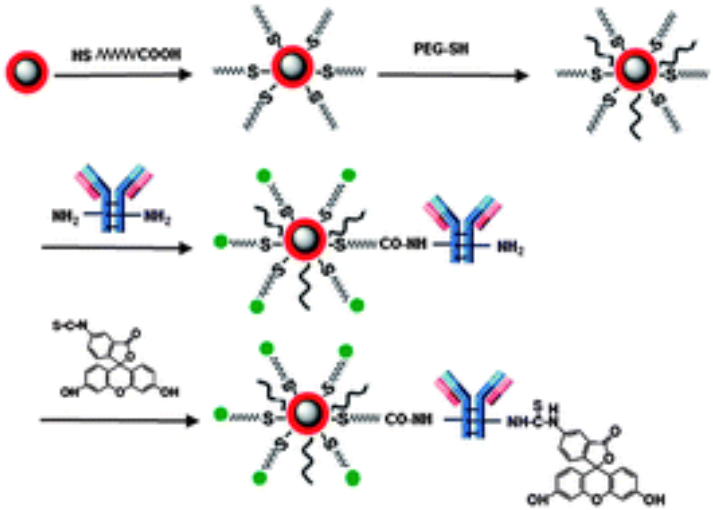

J. Mater. Chem., 2012, 22, 470

core–shell Fe3O4@Au NPs

With the Fe3O4@Au NPs, we can identify the specific location of tumor in the body before surgery with a MRI, and then use fluorescence imaging to find and remove all parts of the tumor during the operation

SPION when conjugated with a fluorescent dye, they can also be used for fluorescence imaging, which has a much higher sensitivity than the MRI imaging

MNP: magnetic hyperthermia

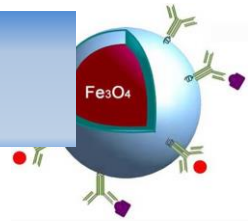

Current Drug Metabolism,
Volume 17 , Issue 8 , 2016

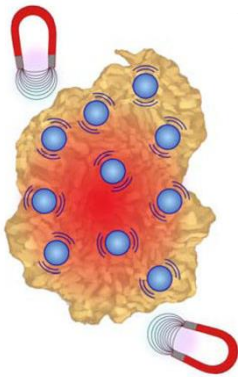

The innate magnetic properties of SPIONs may be harnessed to provide localized hyperthermia that induces tumor necrosis by applying an external magnetic field making SPIONs therapeutic without the addition of functional moieties

Revia RA et al. Materials Today Volume 19,Number 3 April 2016

Magnetic Hyperthermia

Therapeutic effect **Drug releasing trigger**

MNP: magnetic hyperthermia

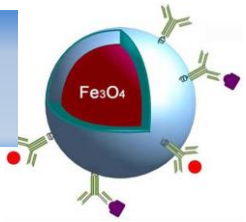

Current Drug Metabolism, Volume 17 , Issue 8 , 2016

PEG-coated magnetite NPs were able to reduce tumor growth through magnetic hyperthermia when intratumorally injected into epidermoid carcinoma xenograft implanted mice

(a) *thermographic infrared photographs taken at different timepoints during magnetitc hyperthermia*

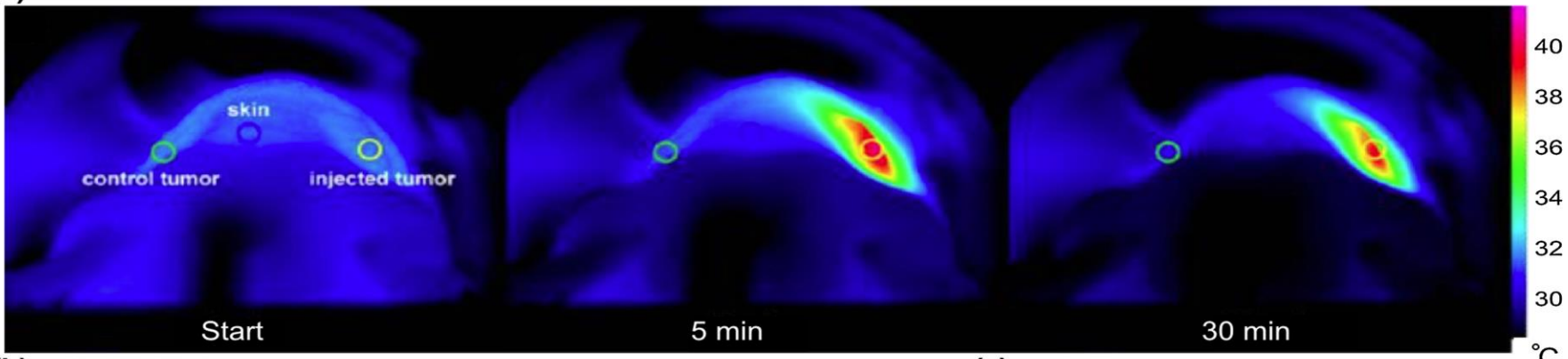

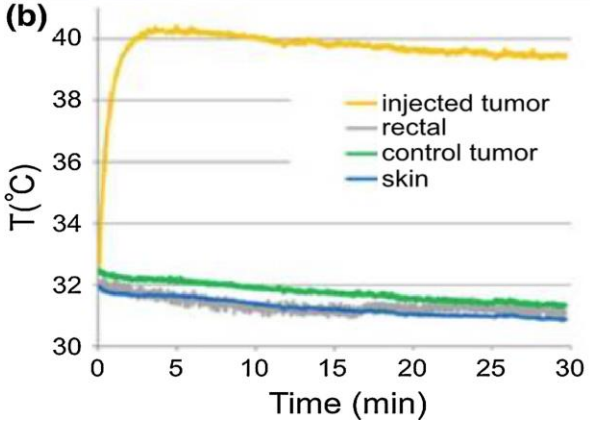

Revia RA et al. Materials Today Volume 19,Number 3 April 2016

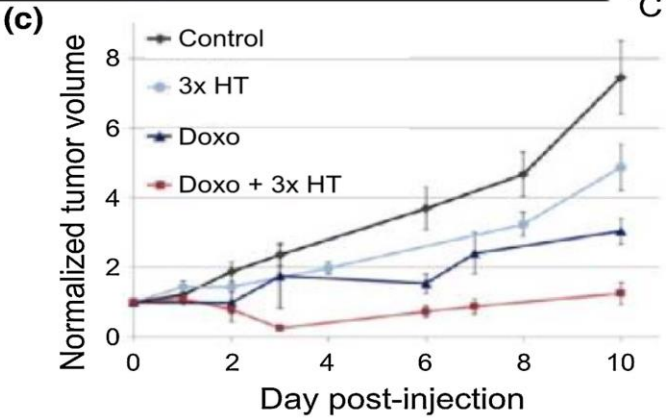

profiles of various organ systems during the magnetic hyperthermia therapy; off-site temperature levels retained normal values whereas the tumor tissue experienced elevated temperatures.

the destruction of the extracellular matrix caused by magnetic hyperthermia led to increased drug penetration

MNPs: Drug release trigger

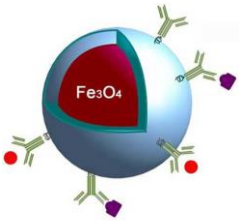

Current Drug Metabolism, Volume 17 , Issue 8 , 2016

Magnetite NP coated with carboxymethyldextran and loaded with doxorubicin

magnetic field

Hua X , Drug Deliv, 2017; 24(1): 511–518

Magnetic hyperthermia effect ca be also used as a drug-releasing trigger. If drugs are encapsulated in a heat labile coating, then controlled release of drugs may be achieved with magnetite NPs when they heat up due to the application of an external magnetic field.

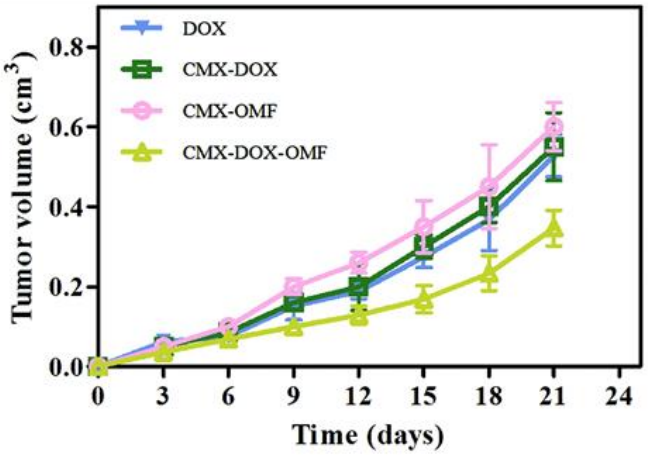

changes in tumor volume over 21 days

MNP: monitoring treatment

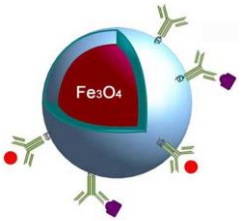

Current Drug Metabolism, Volume 17 , Issue 8 , 2016

Drugs loaded onto iron oxide NPs and then coated in a pH sensitive polymeric coating

Drugs loaded onto NPs may hinder water's access to NP cores and there by nullifies their ability to alter the relaxation times of protons

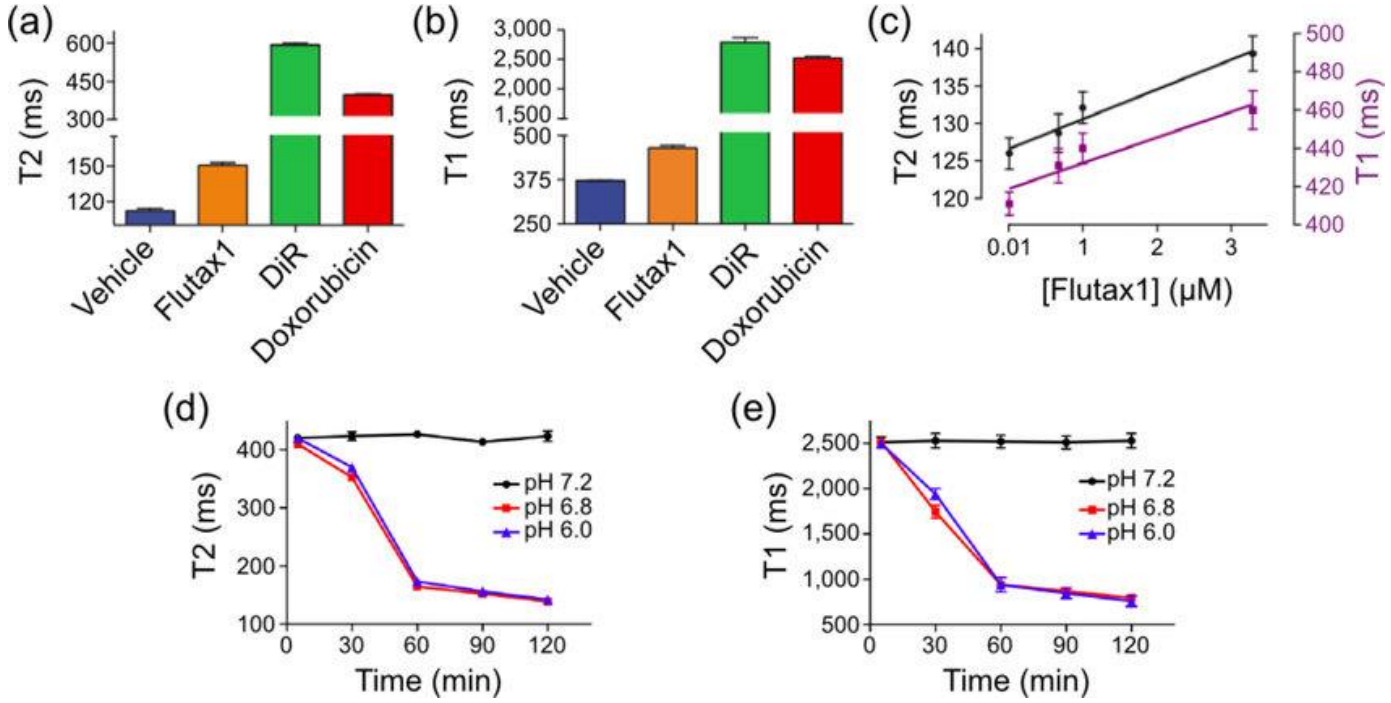

Revia R.A et al.Materials Today 19,Number 3 April 2016

Doxorubicin loaded NPs released the drug when exposed to pH environments of 6.8 or less, and drug release consequently reduced the T1 and T2 values of the NPs. This demonstrates how MRI may be used to monitor cargo release from iron oxide NPs.

Metallic NPs in imaging and therapy

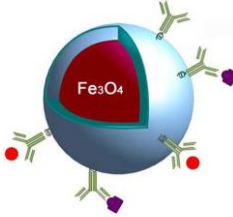

Current Drug Metabolism, Volume 17 , Issue 8 , 2016

NP Core Composition	NP Coating	Hydrodynamic size	Loaded Drug	Targeting Ligand	Cell/In Vivo Model	Application	Ref
Bismuth-iron oxide composite	Dextran	98 nm	None	None	Human liver carcinoma cells (Hep G2) BJ5ta fibroblasts C57BL/6J mice	Dual CT and MRI T2 contrast agents were successfully deployed in an in vivo murine model	41
Iron oxide	PEG	10 nm	None	None	J774 macrophages	SPIONs capable of enhancing T1 contrast in MRI were developed and tested in vivo	45
Iron oxide	None	35 nm	None	Anti-prostate specific membrane antigen J591 antibody	LNCaP cells (CRL-1740) DUI145 cells (HTB-81)	MRI T2 contrast agents that specifically target prostate cancer cells were developed	48
18F-iron oxide	Dextran	30 nm	None	None	BALB/c mice	Trimodal imaging contrast agents providing MRI, PET, and CT capabilities were evaluated in vivo	59
Iron oxide	Dextran	40 nm	Flutax1 DiR Doxorubicin	None	LNCaP cells Mice with PC3 flank xenografts Mice with BT20 flank xenografts	Drug delivery vehicles that release their therapeutics in mildly acidic environments were created; these particles also exhibit changes in MR relaxivity values upon drug release and may thus be used to monitor drug delivery	66
Iron oxide	Chitosan	50 nm	Temozolomide	Chlorotoxin	Glioblastoma cells (U-118 MG) C57BL/6J mice	Drug delivery vehicles capable of carrying the chemotherapeutic temozolomide specifically to glioblastoma brain cancer cells were tested in vitro	70
Iron oxide	PEI	100 nm	siRNA targeting human telomerase reverse transcriptase	None	MCF-7 cells PC3 cells SKOV-3 cells Hep G2 cells BALB/c mice with Hep G2 xenograft tumors	Redox-sensitive gene and siRNA delivery was achieved in vitro and in vivo to induce apoptosis and inhibit growth of liver cancer	77
Iron oxide	Chitosan PEG PEI	40 nm	Apurinic endonuclease 1 suppressing siRNA	None	Medulloblastoma cells (UW228-1) Ependymoma cells (Res196)	In vitro delivery of siRNA to two types of brain tumor cells was facilitated by iron oxide NPs; the siRNA reduced the activity of an enzyme implicated in radiation resistance in tumors	79
Iron oxide	PEG	19 nm	None	None	Immunodeficient athymic NMRI mice Human epidermoid carcinoma xenografts (A431 cells)	SPIONs injected intratumorally into skin cancer xenografts induced localized hyperthermia when irradiated with an external magnetic field, arresting tumor growth	83
Iron oxide	PEG	75 - 200 nm	Doxorubicin Paclitaxel	IVO24 peptide	Human cervicalcarcinoma cells (HeLa)Human breast carcinoma cells (MCF-7)Mice bearing MCF-7tumors	Dual-drug loaded, therapeutic delivery vehiclesthat release drugs upon exposure to an externalmagnetic field were used to treat breast and cervical cancer models in vitro and in vivo	84
Gold-ironoxidecomposite	PEG	25 nm	None	A33 scFvantibody	Colorectal cancer cells(SW1222 and HT 29)	Active targeting of colorectal cancer cells andsubsequent selective photothermal ablation oftumor tissue in vivo	88
Iron oxide	APTES	15nm	Pheophorbide-A	None	Epithelial cancer cells(KB cells)	Simultaneous photodynamic therapy and dual-mode fluorescence/MR imaging of epithelialcancer cells in vitro was demonstrated	94
Iron oxide	PEG	100 nm	Chlorin e6	None	Murine breast cancercells (4T1)BALB/c mice	In vitro and in vivo photodynamic therapy wasused to treat breast cancer in a murine model;cancer tissue was specifically targeted bydrawing NPs to tumor sites via an externalmagnetic field	95

Revia R.A et al.Materials Today Volume 19,Number 3 April 2016

Gold nanoparticle (AuNP)

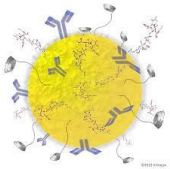

- Medicinal application of gold and its complexes also has a long history.

- The first data on colloidal gold (colloidal suspension of nanoparticles of gold in a fluid) can be found in ancient Chinese, Arabian, and Indian papers from V–IV centuries BC, which recommended it for the treatment of various diseases, although the mechanism of action was poorly understood. In medieval Europe, colloidal gold was frequently studied in alchemist laboratories and used for the treatment of mental diseases, syphilis, diarrhea, and even recommended as the elixir of longevity.

- In the last 40 years several studies are devoted to biomedical applications of gold nanoparticles

AuNP : optical properties

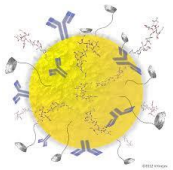

Surface plasmon resonance (SPR) a phenomenon occurs when the frequency of the oscillation of free conductive electrons at the surface of the nanoparticle resonates with the frequency of the incoming light radiation, resulting in a plasmon band.

(A) The electromagnetic field of incident light induces coherent collective oscillation of conduction band electrons. (B) Comparison between nanospheres and nanorods, showing that the dipolar oscillation depends on particle size and shape. While nanospheres show one surface plasmon resonance band, nanorods have two: a strong longitudinal band in near-infrared region (long axis) and a weak transverse band (short axis).

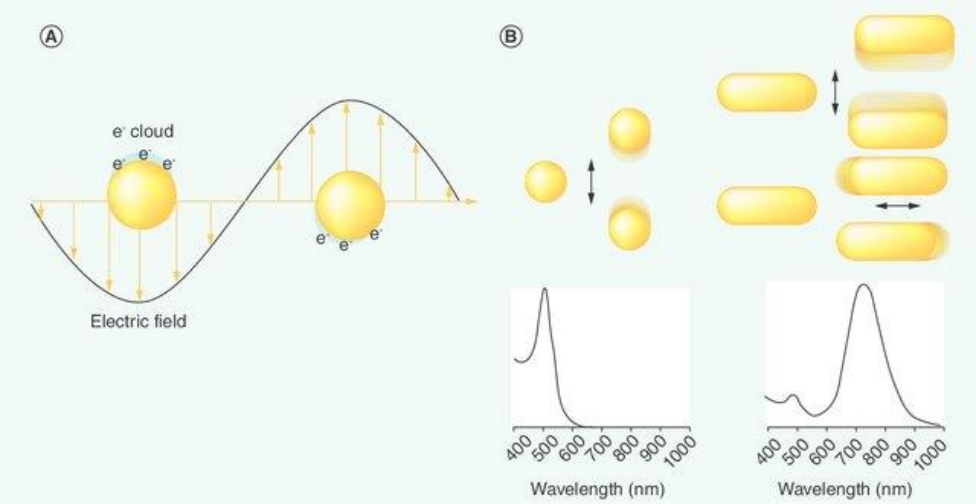

AuNPs provide both absorption and scattering effects, depending on the size and shape but also on the type of solvent, surface ligand, core charge, temperature, and the proximity of other nanoparticles, influencing the electron charge density on the particle surface

AuNP : Photothermal therapy

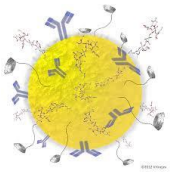

(a)

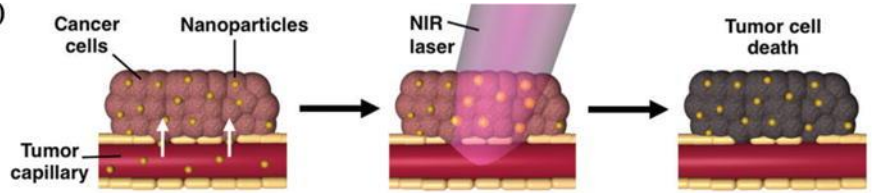

(b)

	Nanoshells	Nanorods	Nanocages	Nanostars
Schematic				
SEM	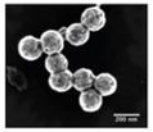	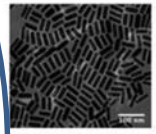	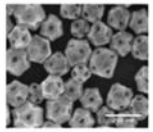	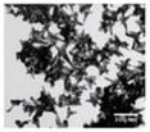
Size for PTT	~150 nm diameter	~10 nm x 40 nm	~40-60 nm length	~45-120 nm
Stage of development	Clinical trials: lung, head & neck, and prostate cancer	Preclinical	Preclinical	Preclinical
Unique features	Core:shell structure	Two resonance peaks	Drug loading capabilities	Large surface area for bioconjugation

- ✓ The irradiation in the range of SPR is followed by rapid conversion of light into heat that causes the disruption of cellular membranes and protein denaturation leading to cell death.
- ✓ The damage on the healthy tissue can be partially overcome by the use of laser radiation enabling the controlled and precise destruction of cancer tissue.
- ✓ Size, shape, and structure greatly influence photothermal properties
- ✓ Near infrared (NIR) light is chosen for PTT due to minimal absorption by the tissues at these wavelengths (650–900 nm)

- ➢ Nanoshells coated with PEG (AuroLase, commercialized by Nanospectra Biosciences, Inc.) are currently the only AuNP for PTT being evaluated in clinical trials

AuNP : Photothermal therapy

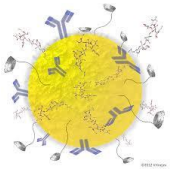

Cooperative nanosystem in mice bearing MDA-MB-435 tumors

Dox-loaded liposomes + AuNR

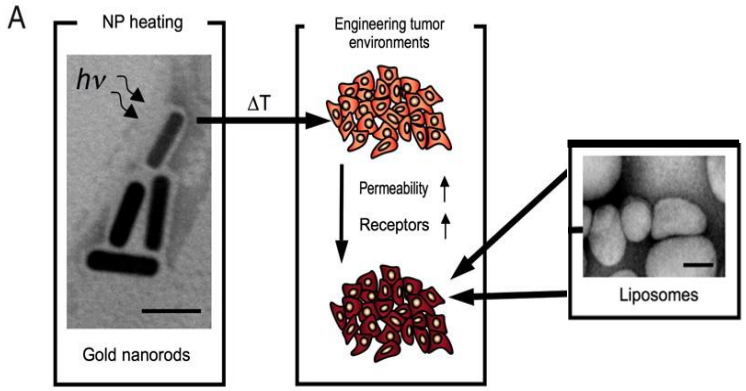

A cooperative system that targeted drug-loaded liposomes to the p32 protein, which is upregulated following NR mediated PTT, to improve tumor delivery of the drugs and enhance treatment outcome versus PTT or chemotherapy individually has been prepared.

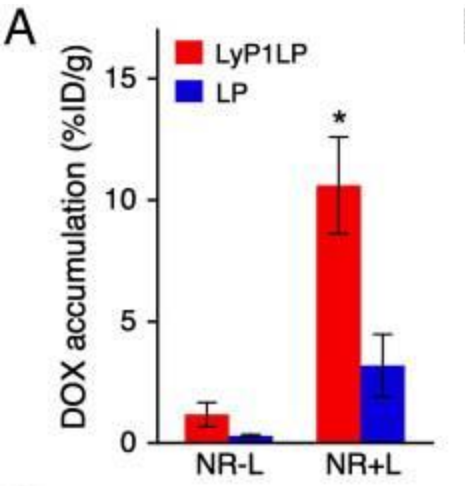

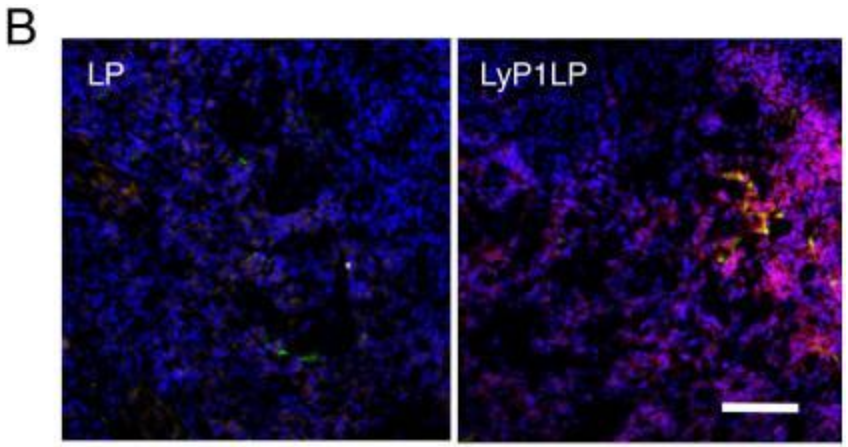

Amount of DOX present was quantified by fluorescence microscopy to yield a percentage of injected dose per tissue mass. (B)

Histological analysis of DOX (Alexa Fluor® 488 label on control liposome and 5(6)-carboxyfluorescein (FAM) label on LyP-1, Green) and DOX (Red)

LyP-1-conjugated liposomes

Non conjugated liposomes

Park J-H, et al. Proc Natl Acad Sci U S A 2010, 107:981–986.

AuNP : Photoacustic imaging

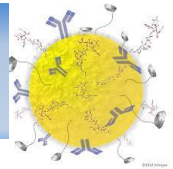

In PA imaging, tissue is irradiated with a pulsed laser and light absorption produces a temperature rise in the tissue leading to its subsequent thermo-elastic expansion. The pressure induced by this expansion leads to propagation of acoustic waves, which are detected by an ultrasound transducer at the surface of the body

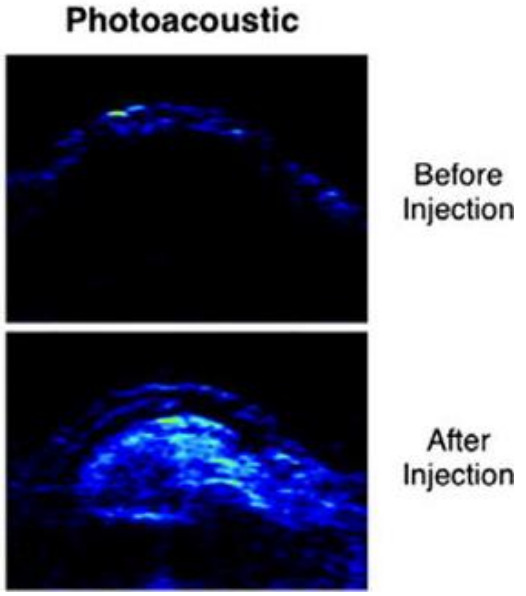

WIREs Nanomed Nanobiotechnol 2017, 9:e1449

photoacoustic images demonstrate enhanced signal from biodegradable gold-based NPs accumulated within the tumor. NPs were composed of clusters of small gold nanoparticles that produced an ultrastrong plasmonic coupling effect for imaging and PTT.

AuNP : Photodynamic therapy

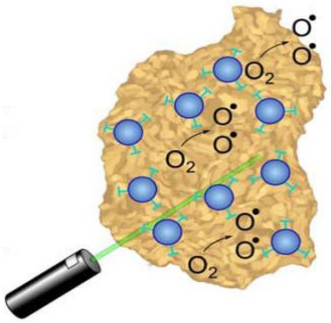

Vankayala R., Biomaterials 2014, 35, 5527-5538

Metal nanoparticles find application as photosensitizers in photodynamic therapy (PDT). It is an alternative cancer treatment modality, which, in principle, is far more effective than PTT, where every singlet O2 molecule can facilitate the destruction of cancer cells, and, unlike PTT effect, will not be suppressed by low temperatures

Most of the organic photosensitizers used in clinical PDT treatments are, however, restricted to be activated only by UV and visible light, which has very poor tissue penetration depths and therefore limited to the treatments of surface tumors

In metal nanostructures thank to their SPR effect upon photoexcitation, the excited state photon energy can undergo energy transfer to molecular oxygen and generate highly reactive oxygen species, such as singlet oxygen.

AuNP : Photodynamic therapy

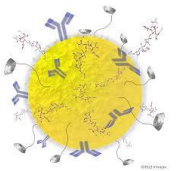

Multimodal systems : PTT and PDT effect

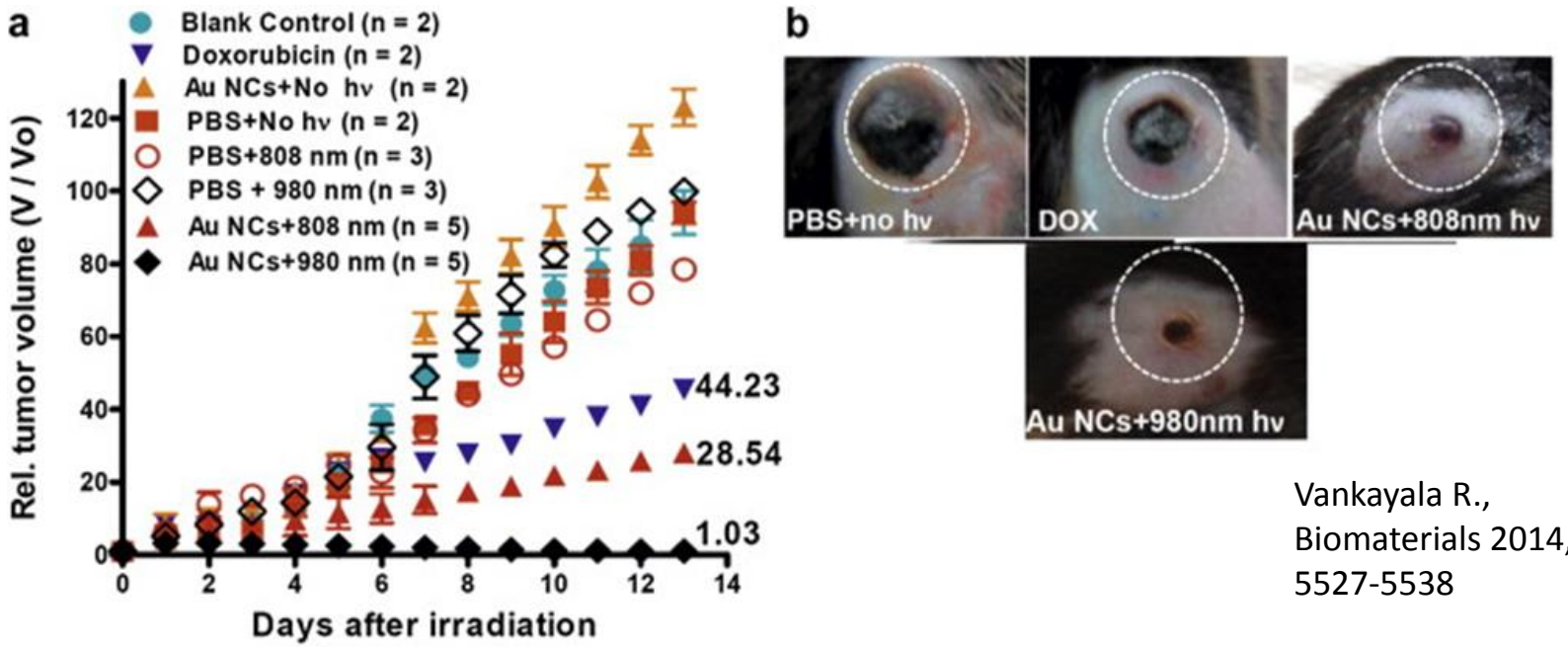

Vankayala R.,
Biomaterials 2014, 35,
5527-5538

In vivo phototherapeutic effects from Au nanocages in B16F0 melanoma implanted mice.
(a) Tumor growth curves of different groups of tumor-bearing mice after treatment. The tumor volumes were normalized to the initial sizes.
b) Representative images of mice showing the sizes of tumors at day 14 after treatment for PBS-injected mice without light, doxorubicin injected mice and lipid-coated Au nanocages injected mice after exposure to 808 and 980 nm laser wavelengths respectively.

Binary Nanocrystalline Heterostructures (BNC)

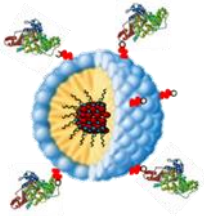

Photodynamic therapy

Hyperthermia

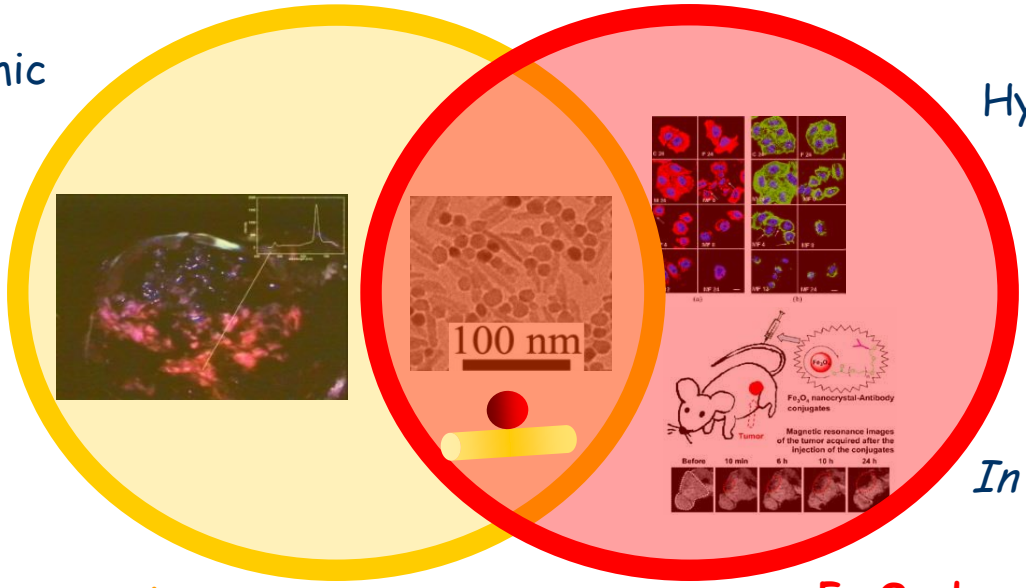

In vivo Imaging

TiO_2 domain

Fe_2O_3 domain

Depalo N, et al, Langmuir. 2011, 27, 6962-70.

BNC: multimodal properties

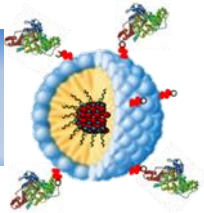

TiO_2

It is among the promising photosensitizer for photodynamic therapy (PDT) against cancer

Semiconductor characterized by excellent photocatalytic activity, low toxicity and high chemical stability.

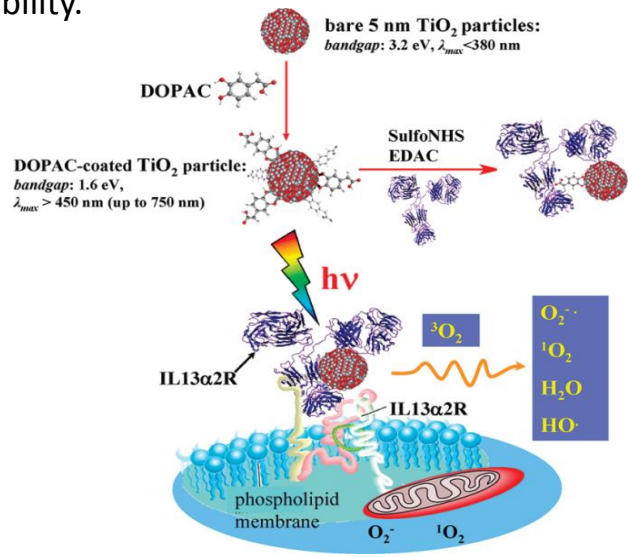

PDT is a form of phototherapy where light-sensitive compounds (photosnesitizers), exposed selectively to light, leads to the formation of powerful oxidative radicals able to destroy the tumor cells.

γ-Fe_2O_3

Superparamagnetic iron oxide NPs show a superior biocompatibility and a greater sensitivity in the micromolar or nanomolar range than other agents, such as gadolinium complexes, in MRI.

Magnetic nanoparticles induce hyperthermia when subjected to an alternating magnetic field of suitable amplitude and frequency.

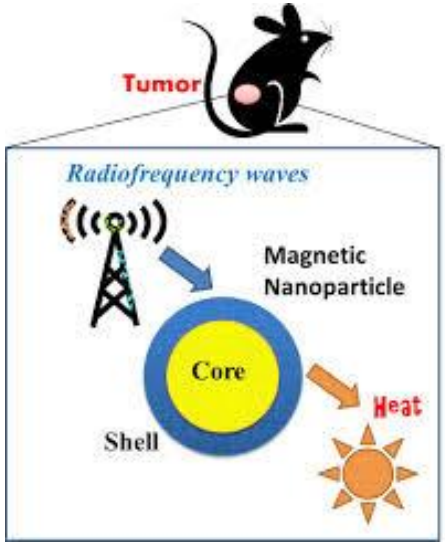

UV-light is brougth into the tumour site using an UV-fiber. Using an on –operation MRI techinique the real –time MRI and in situ PDT could be realized

BNC: synthesis

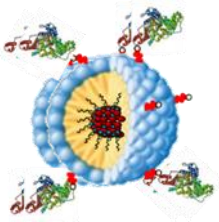

Colloidal chemical approach

1. TiO_2 Nanorods (NRs)

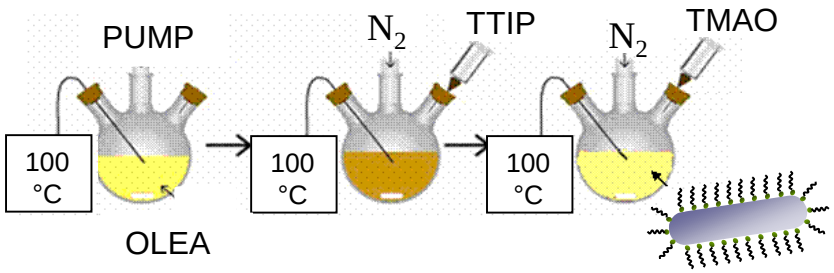

2. TiO_2 -γFe_2O_3 Heterostructures (BNCs)

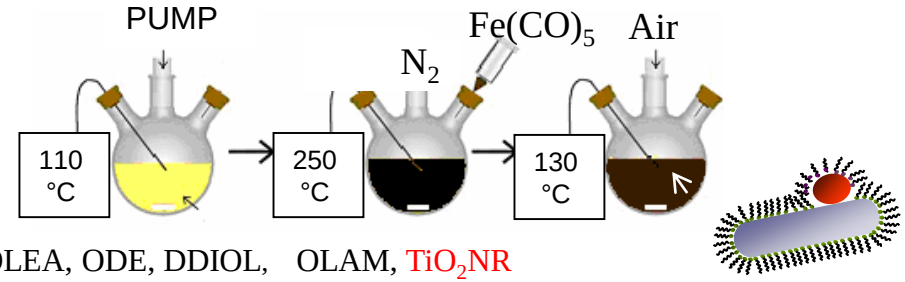

TTIP Titanium Tetraisopropoxide , $Fe(CO)_5$ Iron Pentacarbonyl, ODE 1-Octadecene, OLAM Oleylamine, DDIOL Dodecan-1,2-Diol, TMAO Trimethylamino-N-Oxide, OLEA Oleic Acid

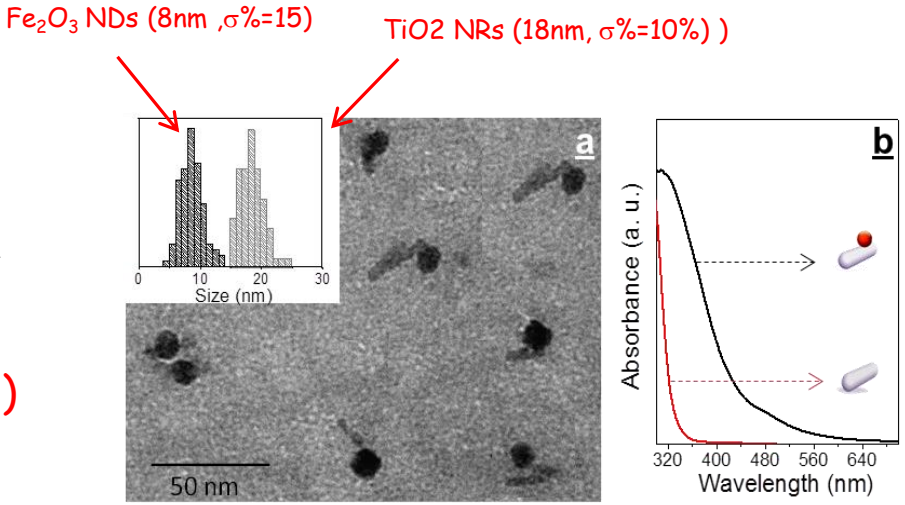

TEM micrograph of organic capped BNCs cast from chloroform (a) Particle size distribution of (gray) TiO2 NRs and (black) Fe2O3 NCs (inset a) NCs.

Absorption spectra of organic capped pure TiO2 NRs and BNCs Enhancement of visible light absorbance

Depalo N, et al, Langmuir. 2011, 27, 6962-70.

BNC: encapsulation in PEG micelle

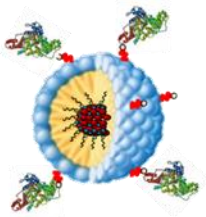

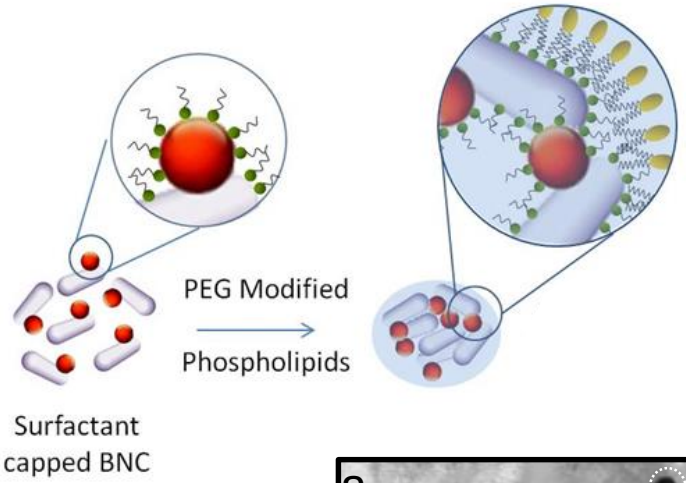

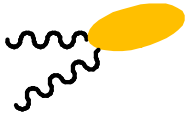

(1,2-Dipalmitoyl-sn-Glycero-3-Phosphoethanolamine-N-[Methoxy(PolyethyleneGlycol)-2000] (PEG-PE) (3.5 * 10-2 M)
1,2-Distearoyl-*sn*-Glycero-3-Phosphoethanolamine-N-[Carboxy(PolyethyleneGlycol)2000] (DSPE-PEG-COOH) (3.5 * 10-2 M)

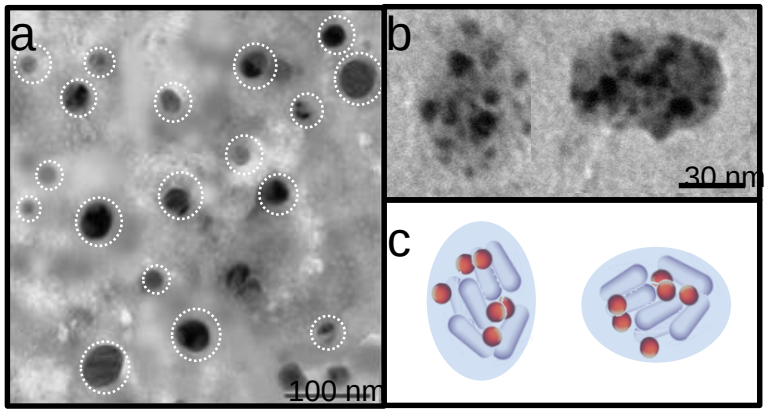

TEM micrographs with positive (a) and negative (b) staining of BNC/Micelles clearly indicates that the micelle diameter ranges from 15 to 70 nm, indicating the formation of aggregates in a wide range of sizes, containing a variable number of BNCs clustered in a single micelle.

Depalo N, et al, Langmuir. 2011, 27, 6962-70.

BNC: active trageting

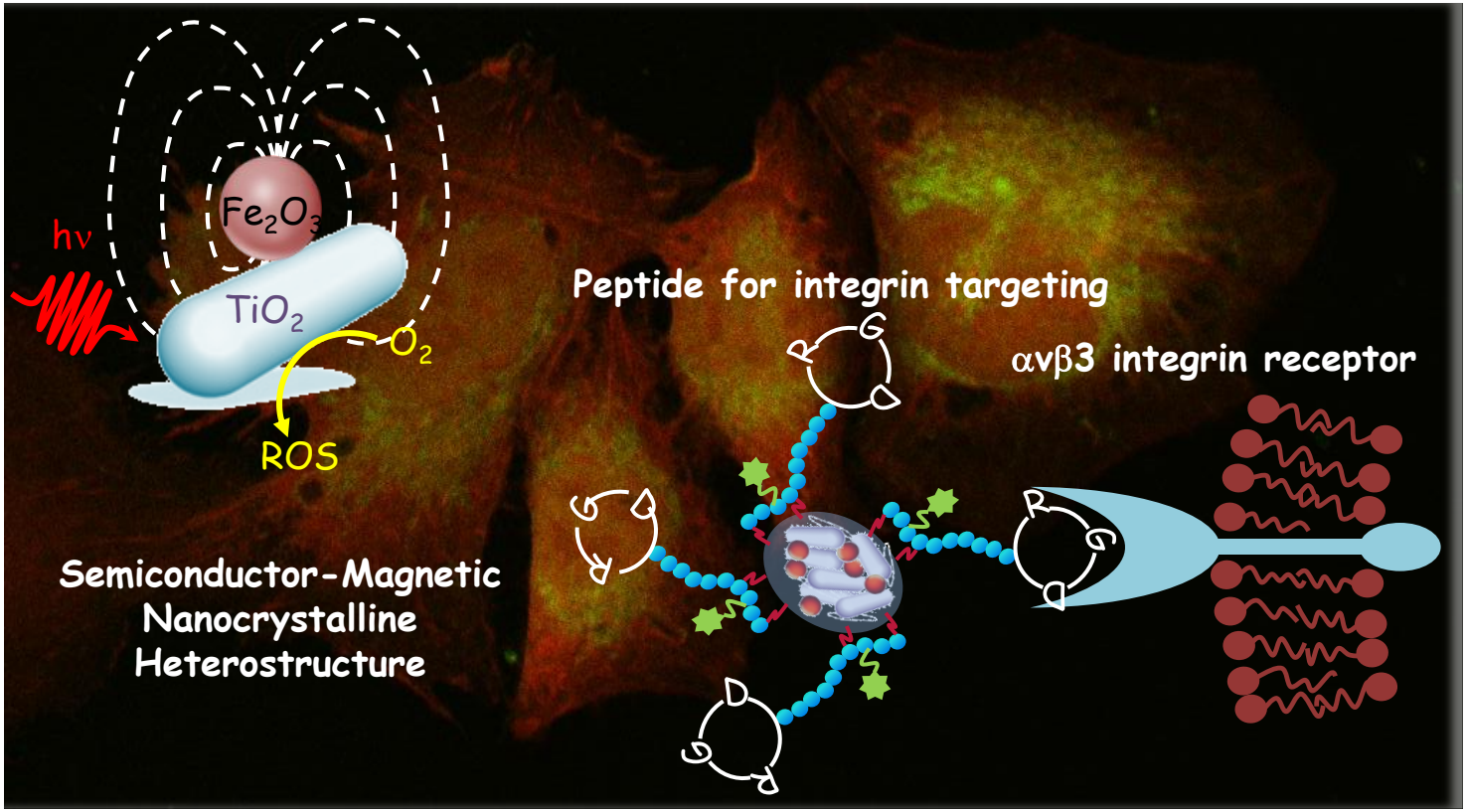

Valente G,. Depalo N., de Paola I., Iacobazzi R. M., Denora N., Laquintana V., Comparelli R., Altamura E., Latronico T., Altomare .M, Fanizza E., Striccoli M., Agostiano A., Saviano M., Del Gatto A., Zaccaro L*. and Curri M. L.*, Nanoresearch, 2016, 644-662.

Integrin receptors

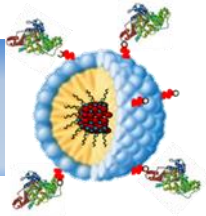

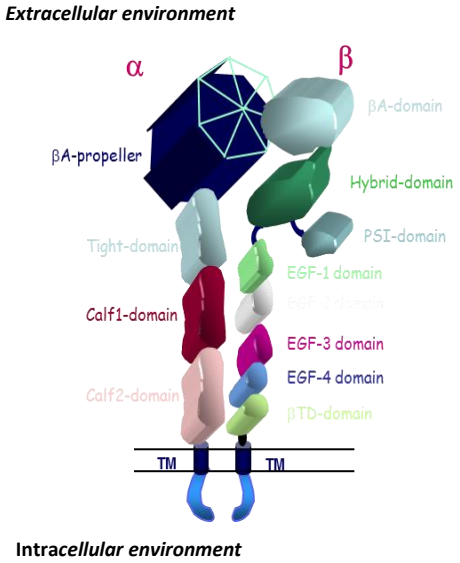

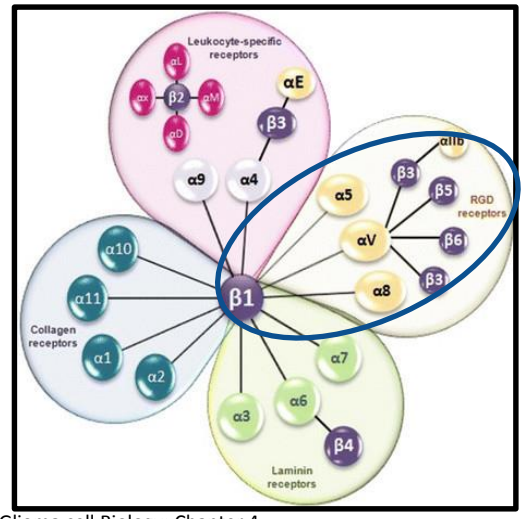

Glioma cell Biology: Chapter 4

Arg-Gly-Asp receptors

✓24 subtype integrins derived by the combination of the different α and β-subunits.

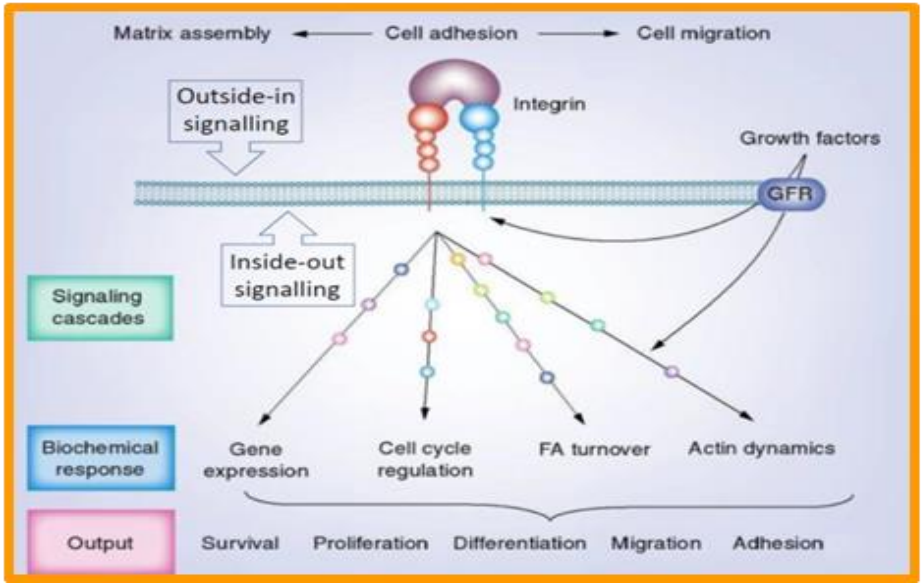

αvβ3 integrin as tumor marker

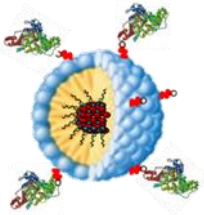

- highly expressed on activated endothelial cells and new-born vessels in tumors, but it is completely absent in the rest of endothelial cells and in most normal organs.
- Its high expression is correlated with tumor invasion and poor prognosis in melanomas, glioma, prostate and breast cancer
- αvβ3 integrin is a marker of cancer stem cells and is associated with epithelial-to-mesenchymal transition
- It is involved in the transformation of drug resistance and tumor recurrence

BNC/Micelle: bioconjugation

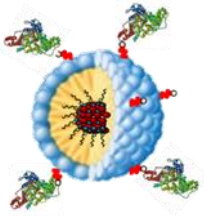

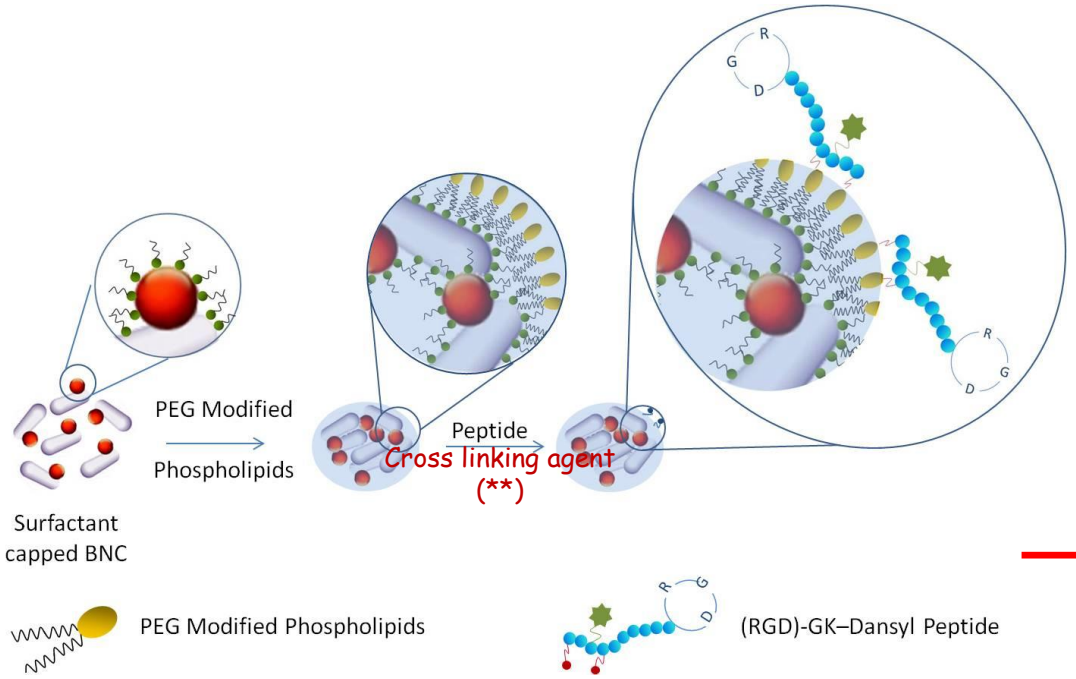

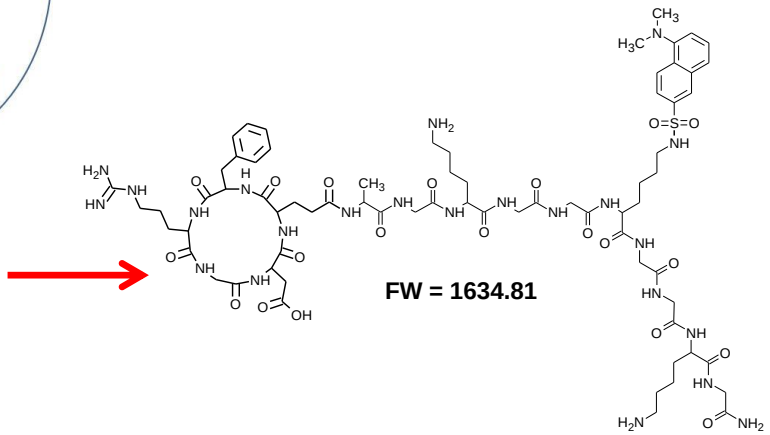

Scheme. EDC/Sulfo-NHS Conjugation Reaction

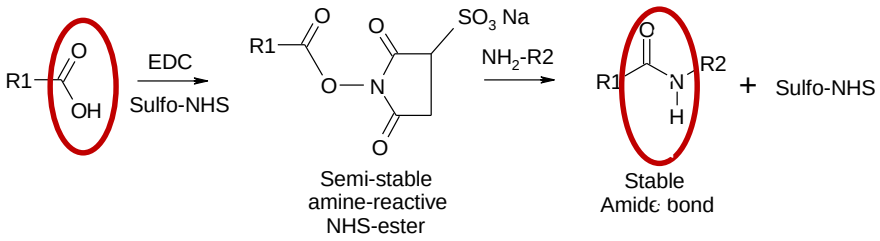

[-COOH] (M)	[EDC] (M)	[SulfoNHS] (M)	[(GK)2DNS Peptide] (M)	$t_{reaction}$ (hr)
5.10^{-4}	5.10^{-3}	$1.25.10^{-2}$	$1.0.10^{-4}$	2
5.10^{-4}	5.10^{-3}	$1.25.10^{-2}$	$1.5.10^{-4}$	2
5.10^{-4}	5.10^{-3}	$1.25.10^{-2}$	$5.0.10^{-4}$	2
5.10^{-4}	5.10^{-3}	$1.25.10^{-2}$	1.10^{-3}	2

(**) 1-Ethyl-3(3-Dimethylaminopropyl)Carbodiimide Hydrocloride (EDC), N-Hydroxysulfosuccinimide (Sulfo-NHS)

Valente G. et al. Nanoresearch, 2016, 644-662.

UV, HPLC, FTIR

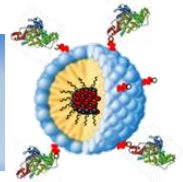

a

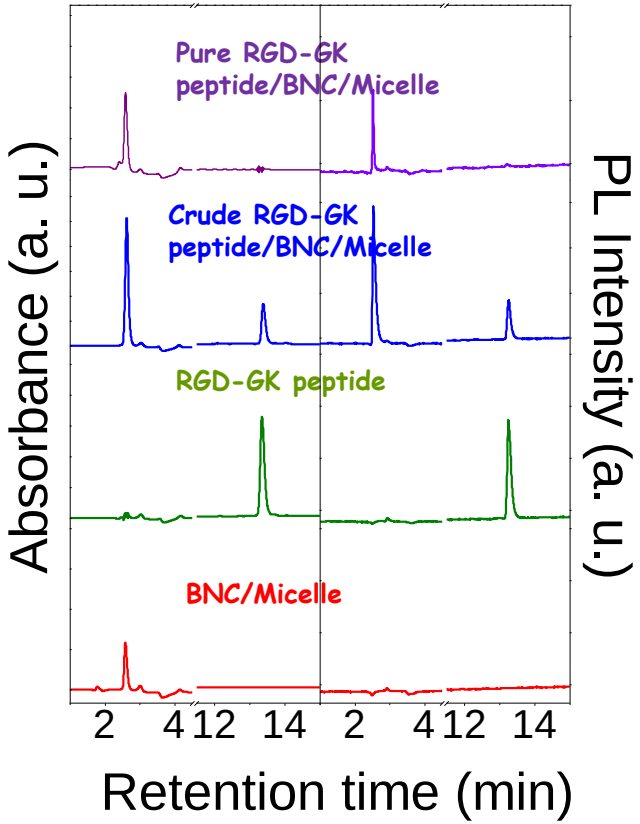

The efficiency of purification has been investigated by means of HPLC analysis, using UV-Vis and fluorescence detectors. The PL signals has been recorded at 560 nm (λ ex= 329 nm)

b

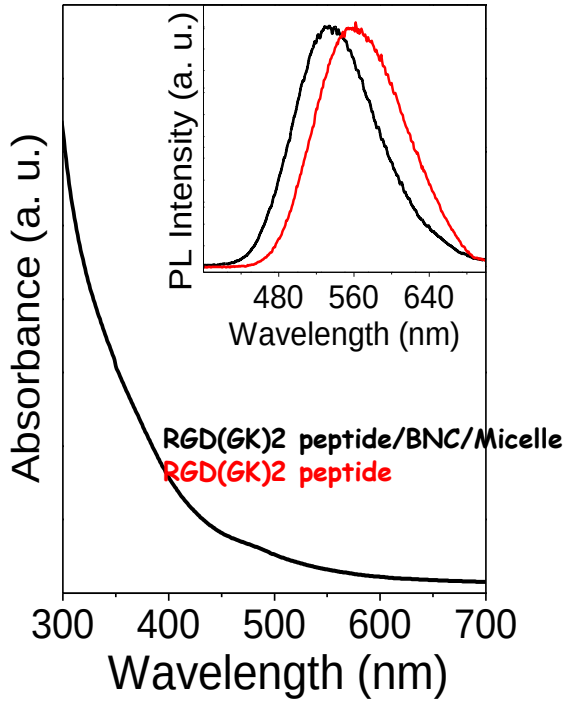

The shift of emission maximum wavelength from 560 nm to 532 nm assigned to the micellar environment around the probe, which is particularly sensitive to any polarity change of the surrounding medium

c

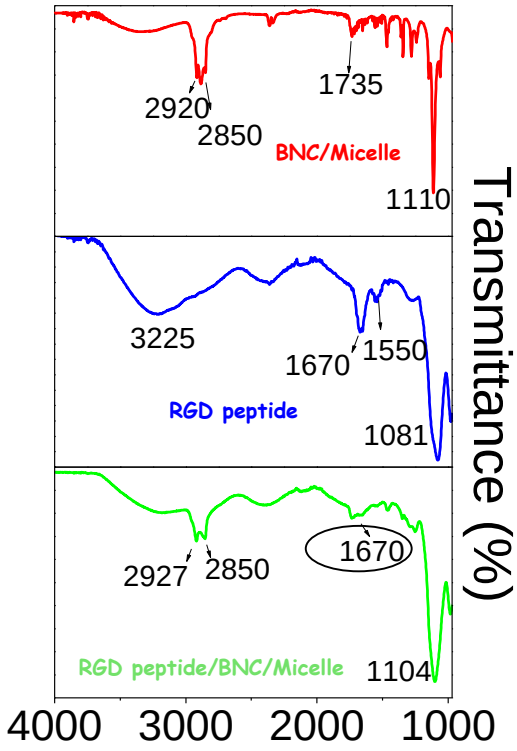

The presence of Amide I mode band in the peptide/BNC/Micelle spectrum confirms the occurrence of the bioconjugation reaction.

[RGD(GK)2- peptide] conjugated to BNC/micelle surface has been estimated, by PL measurements, to be 98 ± 4 μg/mL,

Valente G,. Depalo N., de Paola I., Iacobazzi R. M., Denora N., Laquintana V., Comparelli R., Altamura E., Latronico T., Altomare .M, Fanizza E., Striccoli M., Agostiano A., Saviano M., Del Gatto A., Zaccaro L. and Curri M. L., Nanoresearch, 2016, 644-662.

Dynamic Light Scattering

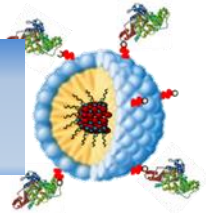

monomodal size distribution

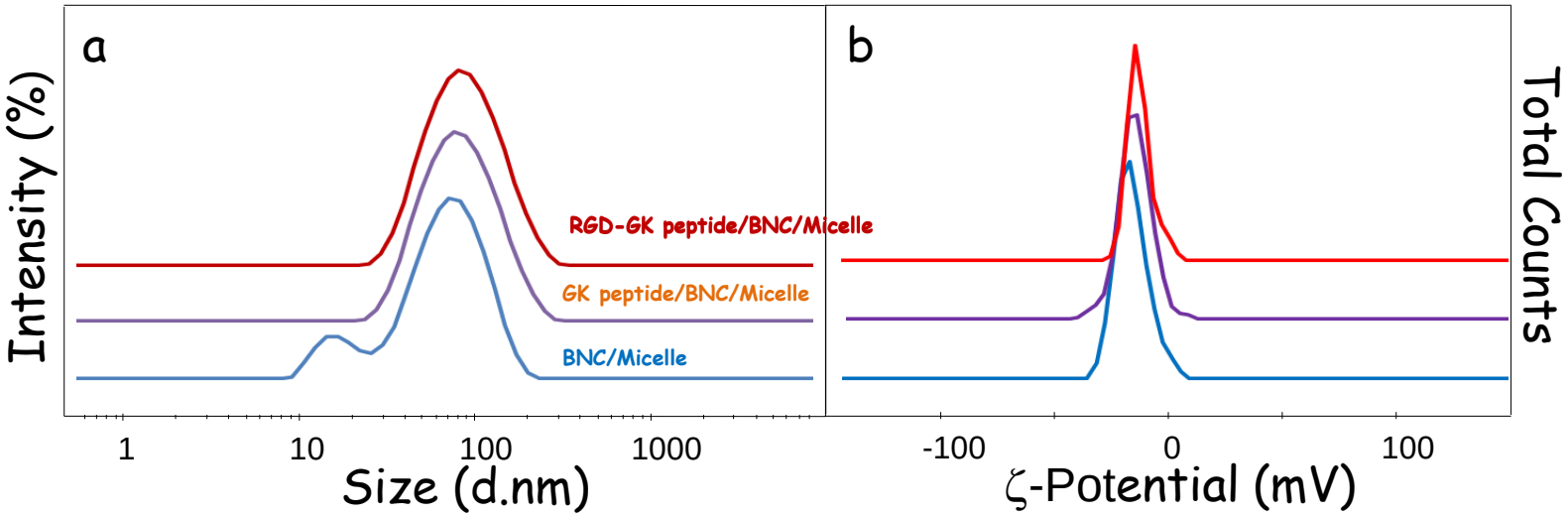

81 nm (PDI = 0.108 ± 0.003)
80 nm (PDI = 0.188 ± 0.002)

-17.1 ± 0.9 mV
-16.6 ± 0.26 mV

Valente G. et al. Nanoresearch, 2016, 644-662.

Citoxycity studies

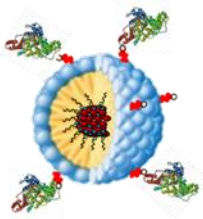

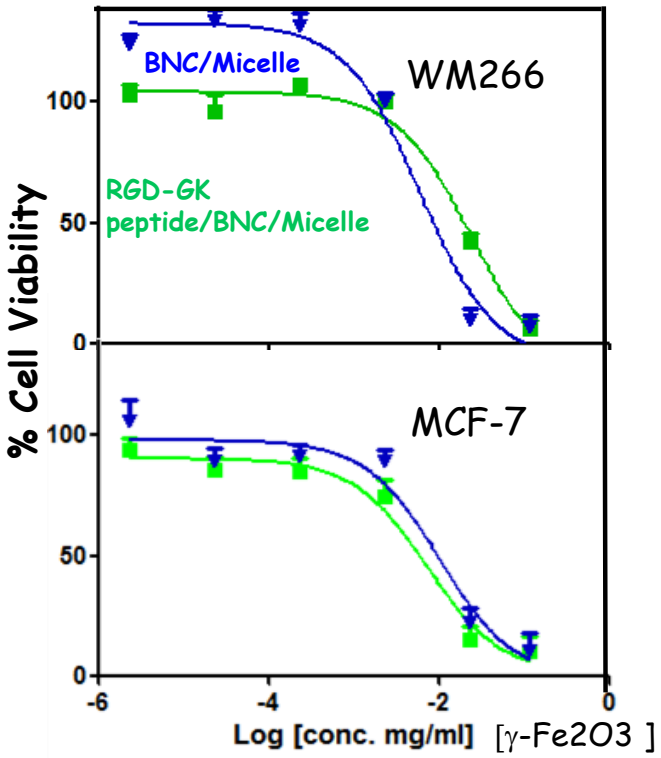

Incubation with γ–Fe_2O_3 concentration values ranging from $2.27*10^{-6}$ to 0.113 mg/mL (TiO_2 concentration range from $2.93*10^{-2}$ to $5.87*10^{-7}$ mg/mL) for 72 hours.

At γ–Fe2O3 concentration values ranging from $2.27*10^{-6}$ to $2.27*10^{-4}$ mg/mL no significant effect on cell viability can be observed

Cell Line	IC50 (mg/mL)	
	BNC/Micelles	RGD(GK)2 - Peptide/BNC/Micelle Conjugates
MCF-7	0.0095± 0.0020	0.0055 ± 0.0032
WM266	0.0076± 0.0030	0.0190 ± 0.0027

IC50 values expressed as γ-Fe_2O_3 concentration.
In WM266 cells the cytotoxic activity of RGD(GK)2/BNC/Micelle conjugates has been found slightly lower than that of BNC/Micelles

Valente G,. Depalo N., de Paola I., Iacobazzi R. M., Denora N., Laquintana V., Comparelli R., Altamura E., Latronico T., Altomare .M, Fanizza E., Striccoli M., Agostiano A., Saviano M., Del Gatto A., Zaccaro L. and Curri M. L., Nanoresearch, 2016, 644-662.

Confocal microscopy

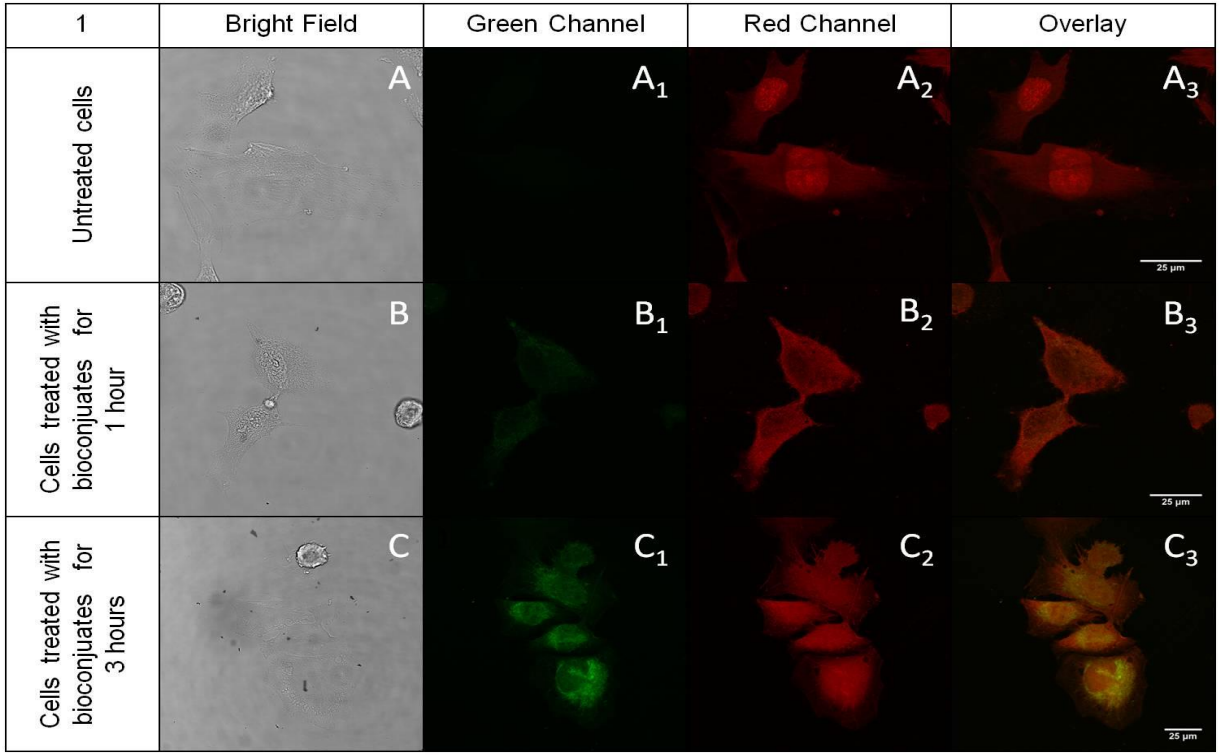

The cells have been incubated with conjugate samples at concentration of $2.27*10^{-3}$ mg/mL for 1 and 3 hours fixed and treated with Phalloidin-TRIC, able to stain the F-actin cytoskeleton of the cell.
Scale bar 25 µm

Valente G,. Depalo N., de Paola I., Iacobazzi R. M., Denora N., Laquintana V., Comparelli R., Altamura E., Latronico T., Altomare .M, Fanizza E., Striccoli M., Agostiano A., Saviano M., Del Gatto A., Zaccaro L. and Curri M. L., Nanoresearch, 2016, 644-662.

Silica coated SPION decorated with Au seeds

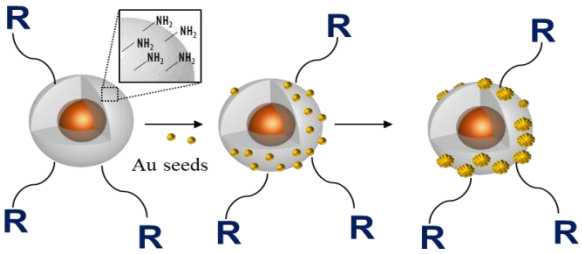

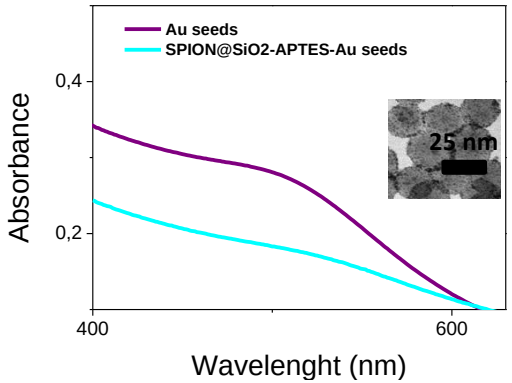

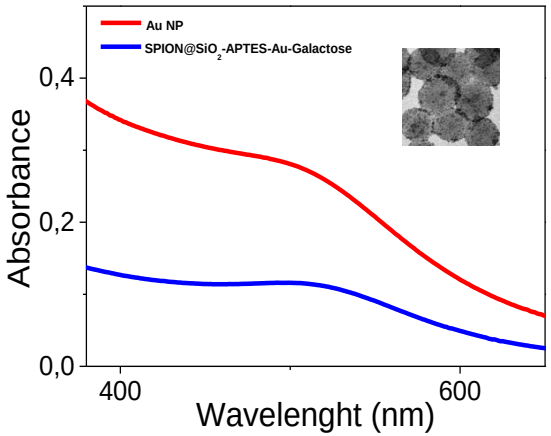

asialoglycoprotein receptor tumor marker overexpressed in hepatocarcinoma


!
Thank you
for your
attention!